ADVANCES IN INORGANIC CHEMISTRY, VOL. 36

PROBING STRUCTURE–FUNCTION RELATIONS IN FERRITIN AND BACTERIOFERRITIN

P. M. HARRISON, S. C. ANDREWS, P. J. ARTYMIUK, G. C. FORD, J. R. GUEST, J. HIRZMANN, D. M. LAWSON, J. C. LIVINGSTONE, J. M. A. SMITH, A. TREFFRY, and S. J. YEWDALL

Department of Molecular Biology and Biotechnology, The Krebs Institute, The University, Sheffield S10 2TN, England

I. Introduction

Inorganic biochemistry (bioinorganic chemistry) has developed rapidly in the last 15 years and Professor R. J. P. Williams has played a very major part in its development. He was among the first to stress the importance in biology of metal ions and other species traditionally considered to be "inorganic." Such processes range from the regulation of gene expression and other control mechanisms, to those involving catalysis, redox change, and biomineralization (*1–4*). To maintain and integrate all such processes, there must be tightly controlled homeostatic mechanisms regulating the concentration of the free ions both

within cells and in the extracellular fluids of the larger multicellular organisms (*4*).

Iron, because of its abundance and versatility, has become an essential element for virtually all forms of life. It is found in enzymes with a variety of functions, e.g., ribonucleotide reductase, aconitase, nitrogenase, catechol dioxygenase, acid phosphatase, and procollagen proline hydroxylase, and in several of the electron transfer proteins of respiration and photosynthesis. Examples of iron biomineralization are found in the formation of magnetic iron oxides or sulfides that give magnetotatic bacteria their ability to swim along magnetic lines of force (*5, 6*), and in the deposition of radular teeth in the marine molluscs that enables them to scrape food off hard rock surfaces (*7*). It also appears that iron may be the prosthetic group of fumarate nitrate reductase (FNR), a transcriptional regulator for oxygen-dependent gene expression in *Escherichia coli* (*8*).

The need for iron, coupled with the low solubility of Fe(III), has led to the production by most microorganisms of iron scavengers, or siderophores (*9*). The synthesis of the siderophore aerobactin in *E. coli* involves several proteins encoded in an operon downstream from a promoter that is regulated by the protein, ferric uptake regulation (FUR). The Fe(II) acts as the corepressor of the *fur* gene, transcription of the genes encoding the proteins required for iron uptake being switched on by low levels of Fe(II) (*10*). Bacterial ferritin (bacterioferritin, or BFR) may also be involved in regulating levels of free iron within the cell once the iron has been taken up. This is important not only because of iron's involvement in many physiological processes, but because of another aspect of iron's biochemistry: unbridled iron can lead to damage of cell constituents through its ability to catalyze the formation of reactive hydroxyl radicals. These toxic effects may be avoided by sequestration in bacterioferritin, or in the ferritin of eukaryotes.

Ferritins present several of the features of iron biochemistry mentioned above. They sequester iron in a safe form as a hydrous ferric oxide–phosphate mineral inside a protein coat. The protein, a hollow shell, has a capacity for up to about 4000 Fe atoms by virtue of its ability to pack this iron in its interior in a mineral form (*11*). The molecular design renders an otherwise insoluble mineral "soluble" and, by enabling iron to traverse the shell, allows a relatively high surface area of mineral to equilibrate with cytosolic iron. In eukaryotes, iron acquisition and release by ferritin may be to some extent compartmentalized. In higher organisms, iron may be deposited

within ferritin not only for its later use within the same cell, but in some cells, e.g., hepatocytes and embryonic red cells, iron stored in ferritin is a reserve that may be utilized by other cells (*12, 13*). Mineralization in ferritins is a redox process. This has been demonstrated *in vitro* (*14, 15*) and it is likely to be similar *in vivo*. Very recently a redox center responsible for the catalysis of Fe(II) oxidation has been identified in ferritin (*16*). This center is highly conserved in ferritin heavy (H) chains, but its absence from light (L) chains does not prevent iron sequestration. This presents something of a paradox, because it is the synthesis of L subunits that increases most dramatically on iron loading (*12, 13*). However, a high speed of iron sequestration may not be the hallmark of an iron storage protein. Other properties relating to protein turnover or iron availability may be of greater significance. Control of ferritin synthesis by iron is an important aspect of iron homeostasis. Translational control of ferritin synthesis by iron was established (*17*) before an effect on transcription was recognized (*18*). One of the most fascinating aspects of iron metabolism currently undergoing intense study is the mechanism by which iron stimulates ferritin translation and at the same time switches off translation of the transferrin receptor (thereby decreasing cellular iron uptake). The information for this regulation is given in the mRNAs encoding each of these proteins: similar stem–loop structures (iron-responsive elements) in the 5′-untranslated region (UTR) of ferritin mRNAs (both L chain and H chain messages) and in the 3′-UTR (five copies) of the transferrin receptor mRNA are recognized by the same binding protein. At low iron levels, binding of this protein is thought to interfere with the action of nucleases responsible for degradation of the receptor mRNA and to prevent binding of the ferritin mRNA to ribosomes and therefore to repress translation (*19–22*). Iron-responsive elements like those of eukaryotes (human, rat, chicken, and bullfrog) have not been found in bacteria, nor is there an "iron-box" sequence similar to that recognized by FUR, in the promoter region of the bacterioferritin gene *bfr* of *Escherichia coli* (*98*). The question of how bacterioferritin synthesis is regulated has yet to be answered.

For a more detailed discussion of ferritin biosynthesis and the possible physiological roles of isoferritins of different subunit compositions, the reader is referred to the recent literature (*12, 13, 16, 18–22*). In this paper the structures of the iron cores and protein coats of ferritins and the hemoferritins of bacteria are compared and the current state of knowledge concerning mineralization processes in these molecules is discussed in relation to this structural information.

II. Iron Cores of Ferritins and Bacterioferritins

A. Physical and Physicochemical Properties

Animal and plant ferritins (*23*) and bacterioferritins (*24*) give similar low-resolution images in the electron microscope: an electron-opaque "core" (diameter about 60 Å) surrounded by a relatively transparent protein shell (external diameter 100–110 Å). At high resolution, differences are apparent in the iron cores. Horse spleen (*25*) and human spleen (*26*) ferritin cores show large single-domain crystals exhibiting lattice fringes that extend throughout the space available in the protein shell, smaller crystals, or crystals with discontinuities, and cores that contain both crystalline and disordered regions. Selected area electron diffraction (*25, 26*) of these ferritins showed five maxima typical of the mineral ferrihydrite and similar to the product obtained by heating solutions of ferric nitrate (*27*). X-Ray diffraction patterns of bulk ferritin, wet or air dried, or of large single crystals of horse spleen ferritin give similar patterns, which can extend to 0.84 Å (*28*). The strongest reflections, also given by ferrihydrite, are at average spacings, d, of 2.52(s), 2.24(s), 1.98(m), 1.72(w), 1.50(w), and 1.47(s) Å, where the letters s, m, and w denote intensities (strong, medium, and weak, respectively). These can be indexed on a hexagonal cell (a = 5.08 Å, c = 9.40 Å) related to that of hematite, but its lattice contains fewer iron atoms within the interstices of the close-packed oxygen layers, and lateral displacements after four such layers prevent the sharing by FeO_6 octahedra of more than one face (*27*). The iron cores of bacterioferritins isolated from *Pseudomonas aeruginosa* or *Azotobacter vinelandii* show no coherent lattice fringes except in very small regions and no evidence of crystallinity from electron diffraction. The cores of *P. aeruginosa,* although relatively low in iron content (~800 Fe atoms/molecule) seem to be composed of a low-density, "spongy" material extending throughout the available space. In contrast, the electron-dense material in iron-poor ferritin molecules is localized in one or more crystalline particles (*29*).

Other physical properties also show that the iron cores of native ferritins and bacterioferritins are different. Mössbauer spectra of ferritins measured as a function of temperature (Fig. 1) show quadrupole split doublets, with an isomer shift typical of Fe^{3+}, gradually being replaced as the temperature is lowered (between about 50 and 15 K) by a magnetic hyperfine spectrum (*30, 31*). The transition temperature, T_B, is lower than the ordering temperature, T_{ord} (240 K) observed for bulk ferrihydrite (*32*), because of fluctuations in the direction of mag-

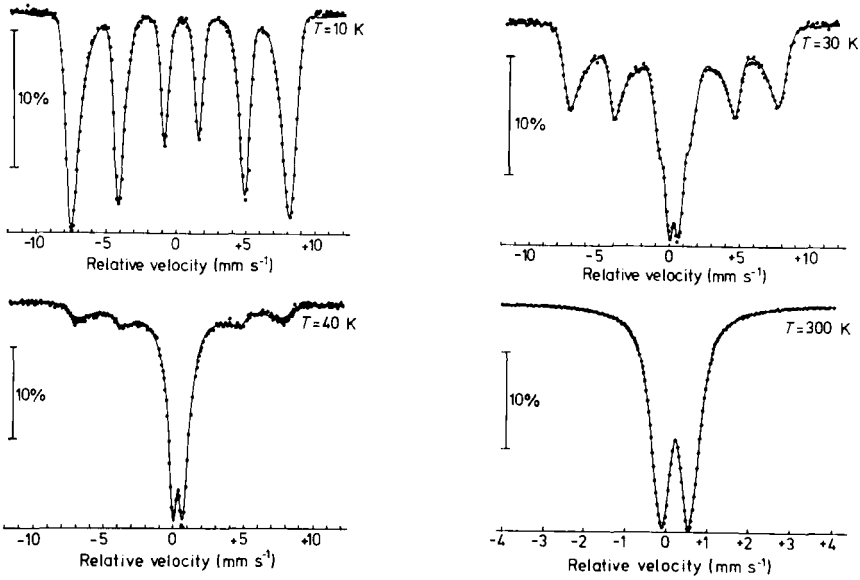

FIG. 1. ^{57}Fe Mössbauer absorption spectra measured for horse spleen ferritin measured at four temperatures relative to a room-temperature ^{57}CoRh source. Reproduced from Ref. *31*. The solid lines represent computer fits to the experimental data. The average blocking temperature, T_B, for this ferritin is near 40 K and the calculated distribution of iron core diameters extends from 36 to nearly 90 Å, with a maximum at 63 Å.

netization resulting from the small particle size of ferritin iron cores. The distribution of T_B values is due to the distribution of particle sizes present in ferritin preparations of variable iron contents. Particle size distributions in horse spleen ferritins have been calculated from the magnetic hyperfine field distributions at different temperatures (*31*). In contrast to ferritin, BFRs from *E. coli* (*33*) and *P. aeruginosa* (*30*) show magnetic ordering only at very low temperatures (near 3 K) (Fig. 2), and the dependence on temperature of the recoil-free fractions giving the Mössbauer spectra suggests that a free magnetic phase transition is taking place (*30, 33*). However, the cores of *A. vinelandii* BFR (*34*) behave more like ferritin, but with a lower average T_B (about 20 rather than 40 K). Liver ferritin from iron-loaded rats, although less well ordered than horse spleen ferritin, shows evidence for superparamagnetism with T_B = 35 K (*35*), and limpet ferritin (*30*) gives a still lower value of T_B, namely 30 K. Both electron-microscopic appearance and Mössbauer spectroscopic behavior suggest significant differences in chemical, structural, and possibly surface properties of the cores in

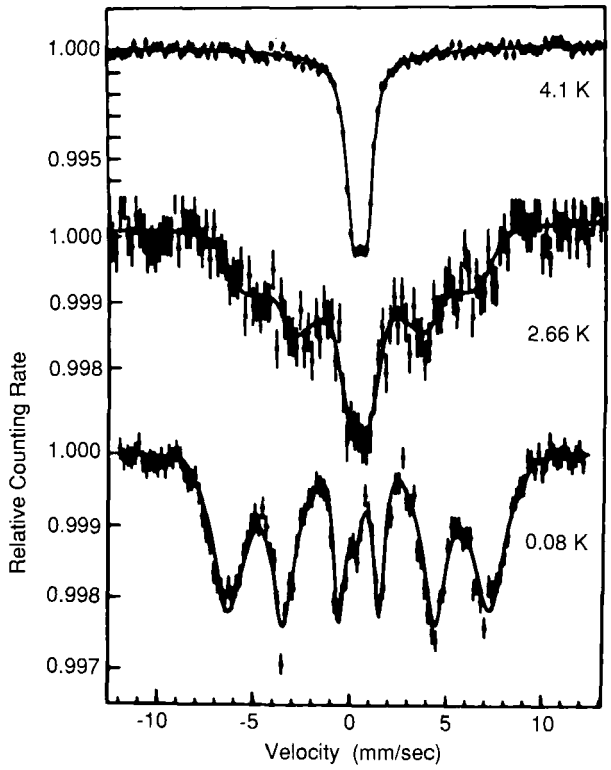

FIG. 2. Mössbauer absorption spectra of the BFR of *Escherichia coli* (grown on media enriched with ^{57}Fe) measured at three temperatures relative to a $^{57}CoRh$ source at room temperature. Reproduced from Ref. *33*.

ferritin and BFR. Differences are also observed in their reduction potentials, namely, -420 ± 20 mV for *A. vinelandii* BFR iron cores in the pH range 7.0–9.0 (*34*) and -390 mV at pH 6.0 compared with -190 mV at pH 7.0, -310 mV at pH 8.0, and -416 mV at pH 9.0 for horse spleen ferritin (*36*). Thus the uptake of protons that accompanies ferritin core reduction (two H^+ per Fe^{3+}) is evident with *A. vinelandii* BFR only at lower pH values. No data are available for other ferritins or BFRs. The *A. vinelandii* BFR heme reduction (*34*) is dependent on the presence of nonheme iron, the midpoint potential being -475 mV for holo- and -225 mV for apo-BFR (where holo and apo apply to the core). Redox potentials are not available for BFR core reduction in the absence of protoporphyrin.

B. Chemical Composition and Crystallinity

Ferrihydrite has the approximate composition $5Fe_2O_3 \cdot 9H_2O$ (*37*). However, ferritin cores contain a substantial, although variable, amount of inorganic phosphate (*38, 39*) (Tables I and II). Earlier analysis of horse spleen ferritin led Michaelis *et al.* (*40*) to propose the formula $(FeOOH)_8(FeO : OPO_3H_2)$, suggesting that some of the hydroxyls of the "ferric oxyhydroxide" were replaced by phosphate. The distribution of phosphate and iron is not uniform among the core particles. In horse spleen ferritin fractionated by density gradient centrifugation, those molecules of lower iron contents contained the higher proportions of phosphate (Table I) (*39*). There is also a considerable variation in iron : phosphorus ratios in different samples (Table II) (*40–43*). At one extreme, no significant amount of inorganic phosphate could be detected in liver ferritin from iron-loaded rats (*35*) and, at the other, high amounts (one P to one to two Fe atoms) were found in two bacterial samples (*26, 34*). The latter cores can probably best be described as hydrous ferric phosphate, the high phosphate being associated with and probably responsible for the poor crystallinity and very low magnetic ordering temperatures. In the ferritins, the reverse is not necessarily true; the cores of both rat liver (*35*) and *Patella laticostata* (*38, 43*) have low phosphate but poor crystallinity, and there are clearly other factors that affect ordering of the mineral structure. One of these is the rate of iron addition. Reconstitution experiments show that gradual build-up by successive small additions gives better ordered cores than those obtained when the same amount of iron is added in a single step (*44*).

TABLE I

Chemical Composition of Horse Spleen Ferritin Iron Cores[a]

Fe atoms/molecule	Fe atoms/phosphate
500	4.5
1200	5.4
1900	7.2
2500	8.7
3000	9.5
3200	11.1
3500	9.8

[a] Data from Ref. *39*.

TABLE II

CHEMICAL COMPOSITIONS AND PROPERTIES OF SOME FERRITINS

Ferritin source	Fe atoms/ molecule	Fe atoms/ phosphate[a]	Fe atoms/ P atoms[b]	Crystallinity	T_B	T_{ord}	Ref.[c]
Human thalassaemia (spleen)	2500	21	20	Good	~40	>50	*26, 43*
Human idiopathic hemochromatosis (liver)	—	9.1	8.7	—	—	—	*41*
Human idiopathic hemochromatosis (liver)	—	3.8	3.0	—	—	—	*41*
Rabbit liver	2900	11.1	—	—	—	—	*42*
Iron-loaded rat liver	3000	Insignificant	36	Fair	~35	>42.5	*35, 38*
Horse spleen	2000	8	—	Good	~40	>40	*31, 39*
Patella laticostata	—	—	33	Poor	~30	~34	*30, 43*
Clavarizona hirtosa	1500	—	13	Poor	~32	~37	*43*
Azotobacter vinelandii	1000	1.5, 1.9	1.7	Amorphous	~18	>20	*34*
Pseudomonas aeruginosa	800	1.7	1.4	Amorphous	>3	~3	*26, 30*
Escherichia coli	—	—	—	—	>3	~3	*33*

[a] Obtained by chemical methods.
[b] Obtained by electron probe microanalysis.
[c] See references for details of methods.

In horse spleen ferritin the relationship between Fe : phosphate and Fe atoms/molecule (Table I), showing that molecules with small cores are relatively rich in phosphate, could mean that much of the phosphate is adsorbed on surface sites or in crystal discontinuities rather than being distributed randomly throughout the core (*39*). This is also suggested by the skewed relationship between phosphate and iron availability: proportionately more of the phosphate is released at the early stages of iron release (*39*). Again the iron and phosphate release behavior and the visible absorption of ferritin that has been incubated with inorganic phosphate after iron core reconstitution suggest it is a better model for native ferritin than for ferritin molecules that have been reconstituted from apoferritin by addition of iron and phosphate together (*39*). Comparison of ferritins reconstituted with and without phosphate shows the former to have a smaller average particle size calculated from chemical analysis (*39*) and Mössbauer spectroscopic measurements (*31*). EXAFS analysis also indicates that, in the former, the iron atoms have a smaller number of iron neighbors (*45*). Further analysis suggests that, in both native *A. vinelandii* BFR and in ferritin iron cores reconstituted with 480 Fe atoms and 120 phosphates/molecule, the iron atoms have five P neighbors on average. In contrast, the

number of P atoms coordinated to Fe was insignificant in native ferritin cores.

Use of labeled amino acids (*17*) or labeled Fe (*46*) has demonstrated that in rat liver the biosynthesis of apoferritin precedes that of ferritin, and the apoferritin shells are gradually filled with iron. Estimates of the cellular concentration of phosphate and iron indicate that the former exceeds the latter by at least three orders of magnitude, and this taken together with the above data suggests that additions of iron and phosphate during ferritin formation are to a large extent kept separate (*39*). Such compartmentalization may not be possible within the bacterial cell and the relatively high phosphate of the BFR may reflect the phosphate concentration in the growth medium. This is likely because the chemical composition and amorphous structure of BFR cores do not result from specific properties of the protein shell. This is shown by the finding that *in vitro* iron core reconstitution by addition of iron in the absence of phosphate gives crystalline ferrihydrite cores resembling those of ferritin within purified *A. vinelandii* and *P. aeruginosa* BFRs (*25*) or in partially purified *E. coli* BFR (*47*).

C. Iron Core Reconstitution in Ferritin and Bacterioferritin

Ferrihydrite cores are reconstituted inside the apoferritin shell *in vitro* by addition of Fe(II) at or near pH 7 in air, sometimes with an added oxidant (*14, 15, 28*). Although, at relatively high Fe concentrations and Fe atoms/apoferritin molecule, some precipitation of ferric oxyhydroxide may occur outside the apoferritin shell, conditions can be chosen wherein this is negligible. Indeed, iron core formation can proceed within the protein under conditions in which no significant Fe(II) oxidation occurs during the time course of the reconstitution experiment in the absence of apoferritin. The thermodynamic driving force for (protein-free) oxidation of Fe(II) at pH 7 (which formally is favored at low pH) is the removal from solution of the product, Fe(III), by hydrolytic polymerization. In principle, apoferritin could promote Fe(II) oxidation, by providing a catalytic oxidation site; hydrolysis, by providing a means of removing protons, and polymerization, by binding Fe(III) atoms at centers suitable for ferrihydrite nucleation (11).

The presence on apoferritin of ferroxidase centers is suggested by four observations: (1) that the initial oxidation step when Fe(II) is added to apoferritin requires a specific oxidant, dioxygen (*48*); (2) that Fe(III) can be produced from Fe(II) in the presence of apoferritin—and intercepted by transferrin under conditions in which hydrolysis is kept

low (*49*); (3) that the rate of Fe(II) oxidation can be drastically reduced when changes are made in the amino acid ligands of a putative ferroxidase center that has been identified by X-ray crystallography of recombinant human H chain apoferritin (rHF) (*50*); and (4) that an initial absorbing species is observed by UV difference spectroscopy when very small numbers (four to eight atoms/molecule) of Fe(II) are oxidized in the presence of apoferritin, under conditions in which oxidation of Fe(II) in the control is insignificant (*51*). The involvement of the protein in ferrihydrite nucleation has been inferred from (1) the finding that it is the early, slow stage of ferrihydrite formation that is accelerated by apoferritin (*15, 52*); (2) the presence of three conserved neighboring glutamates on the inner surface of the protein shell that bind Tb^{3+}, a known competitor for Fe^{3+} (*51, 53*); (3) the analysis of EXAFS data for a 10Fe(III)–apoferritin complex that suggests the presence of 1.3 ± 0.5 atoms of low atomic number in the second Fe coordination shell, which may be carboxylate carbons (*54*). The acceleration of ferrihydrite nucleation could arise from a locally high Fe(III) concentration due to a burst of ferroxidase activity without the provi-

TABLE III

RELATIVE AMOUNTS OF DIFFERENT Fe(III) SPECIES AFTER AEROBIC ADDITION OF $^{57}Fe(II)$ TO HORSE SPLEEN APOFERRITIN[a]

	Fe(III)					
	Solitary		Dimers		Clusters	
Fe atoms/molecule added	%	Atoms/mol	%	Atoms/mol	%	Atoms/mol
4	65	2.6	12	0.5	23	0.9
8	55	4.4	17	1.4	28	2.2
12	40	4.8	25	3.0	34	4.1
20	30	6.0	20	4.0	50	10.0
40	10	4.0	4	1.6	86	34.4
4 ^{56}Fe + 4 ^{57}Fe	35	1.4	27	1.1	38	1.5
4 ^{57}Fe + 4 ^{56}Fe	30	1.2	18	0.7	52	2.1
150 ^{56}Fe + 4 ^{57}Fe	10	0.4	12	0.5	78	3.1

[a] Samples were evaluated at 3 min after addition of $^{57}Fe(II)$, pH 6.4, using Mössbauer spectroscopy. The last three samples represent the addition of either 4 atoms/mole of the Mössbauer isotope, $^{57}Fe(II)$, to molecules already containing either 4 or 150 atoms of a silent $^{56}Fe(III)$ or the addition of 4 $^{56}Fe(II)$ to molecules containing 4 $^{57}Fe(III)$. Note that in all three samples the proportion of Fe(III) found in clusters greatly exceeds that when 4 $^{57}Fe(II)$ are added to apoferritin in air. For further details, see Ref. *57*.

sion of specific nucleation centers, but apoferritin play an active part in both processes.

Once ferrihydrite particles have formed inside the apoferritin cavity they provide alternative oxidation centers for Fe(II) on the iron core particle surface (*15*). Evidence for this includes the following observations: (1) the stoichiometry of Fe(II) oxidation by dioxygen increases from one to approximately four Fe(II)/O_2 as a core formation proceeds (*55*); (2) Fe(II) oxidation can be effected by oxidants other than O_2 once a core is present (*48*); (3) ^{57}Fe(II) can bind directly to core surfaces, as shown by Mössbauer spectroscopy, and the bound ^{57}Fe(II) can be oxidized (*56, 57*); (4) added Fe binds preferentially to any existing iron core clusters rather than to the protein shell, again as shown by analysis of Mössbauer spectra (see Table III and Fig. 3) (*57*); (5) after addition of an excess of Fe(II) to a small Fe(III) core, a $g' = 1.87$ EPR signal

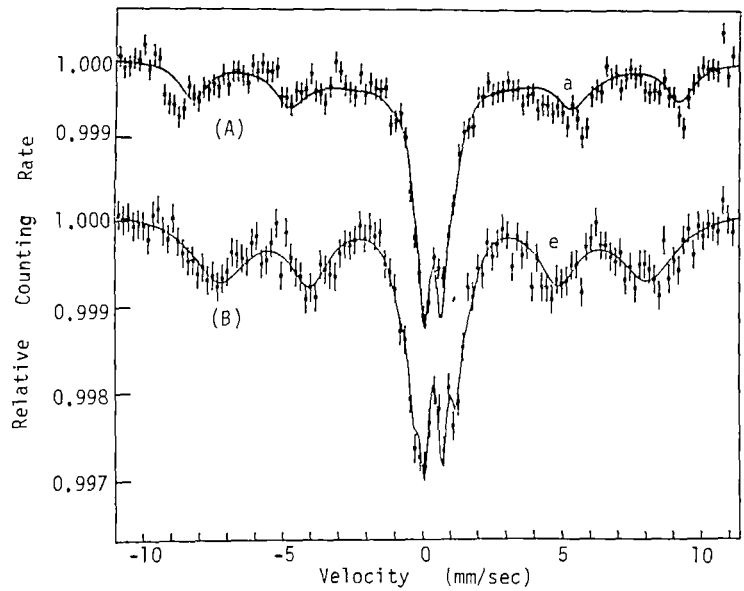

FIG. 3. The 4.1 K Mössbauer spectra of horse spleen apoferritin loaded with iron at pH 6.4 as follows: (A) with four ^{57}Fe/molecule, (B) with four ^{57}Fe/molecule after preloading with 150 ^{56}Fe. Iron was added as Fe(II) in air and samples were frozen 3 min later. (A) The relaxation subspectrum, a, is due to solitary Fe(III) atoms; (B) the magnetic sextet, e, is due to large Fe(III) clusters. Both samples show a central doublet due to small Fe(III) clusters and in B there is a second unresolved doublet due to Fe(III) dimers. All the added iron is Fe(III) at 3 min. At 90 K the sextet, e, of spectrum B, collapses into a doublet, but the subspectrum, a, of spectrum A, is also seen at this temperature. Reproduced from Ref. *69*.

may be observed and this is considered to arise from a mixed-valence binuclear iron cluster (*58*); (6) anaerobic gel filtration experiments have shown that many more Fe(II) atoms bind to ferritin than to apoferritin (*56*). Oxidation of four Fe(II) on iron core surfaces with the reduction of O_2 to water may be an important defense against iron toxicity: Fe(II) initially added to apoferritin seems to yield radical by-products not found at later stages of core growth (*59*).

Some of the intermediates seen by spectroscopic methods during ferritin formation have been mentioned above: an initial UV-absorbing species, which may result from single Fe(III) atoms bound by apoferritin amino acid side chains (*51*); small Fe(III) clusters linked through oxygens and possibly to protein carboxyls responsible for EXAFS spectra (*54*); and Fe(III)–Fe(II) dimers giving characteristic EPR signals (*58*). EPR spectroscopy also shows the presence of single Fe(III) atoms giving a $g' = 4.3$ signal as Fe(II) is added (aerobically or anaerobically) to apoferritin at pH 7.0 and is then allowed to oxidize (*56, 60*). The signal reaches a maximum after about 8–12 Fe atoms/apoferritin have been added (*56, 60*), but remains constant up to at least 100 Fe atoms/molecule (*56*). The fact that it does not continue to increase must be due to the formation of antiferromagnetic clusters in which the Fe(III) is EPR silent (*60*). However, a few of the Fe(III) atoms seem to remain at isolated sites even in the presence of the iron core. It is possible these are in molecules in which iron cores have not nucleated, but it has been suggested they are bound in intersubunit channels (see Section IV).

One of the most informative methods of observing the course of iron core formation, and especially its early stages, is Mössbauer spectroscopy. It can distinguish Fe(II) from Fe(III) as well as a variety of subspectra of both oxidation states: bound and free Fe(II) (*56, 57*); solitary Fe(III) giving relaxation spectra (*57*); Fe(III) in oxo-bridged dimers (*57*); small, nonmagnetic Fe(III) clusters (*57*); and antiferromagnetically coupled Fe(III) in large clusters (*30, 31*). In all of these the different iron environments are reflected in different Mössbauer parameters (Table IV). The relative proportions of the various species obtained under different conditions are shown in Tables III and V. The data are taken from a study in which small numbers of the Mössbauer nuclide ^{57}Fe(II) were added to apoferritin in air and were allowed to oxidize. In some experiments (Table III), ^{57}Fe additions were made to molecules already containing Mössbauer-silent ^{56}Fe. Examples of the various subspectra are given in Ref. *57* and in Figs. 3 and 4. The data in Tables III and V show that under the conditions used, (1) the rate of Fe(II) oxidation is pH dependent, being less at lower pH values, in agreement

TABLE IV

MÖSSBAUER PARAMETERS OF DIFFERENT IRON SPECIES IN HORSE SPLEEN FERRITIN[a]

Species	T (K)	LW (mm/sec)	QS (mm/sec)	IS (mm/sec)	H_{eff} (kOe)	T_r (nsec)
(a) Isolated Fe(III)	90	0.5	—	0.51 (1)	550 (10)	7 (2)
(b) Small Fe(III) clusters	90	0.44 (2)	0.66 (2)	0.50 (1)	—	—
(c) Dimeric Fe(III)	90	0.30 (2)	1.50 (4)	0.50 (2)	—	—
(d) Fe(II)	90	0.45 (2)	3.15 (2)	1.36 (2)	—	—
(d_1) Fe (II)	90	0.30 (2)	3.36 (1)	1.38 (1)	—	—
(d_2) Fe(II)	90	0.44 (2)	3.03 (1)	1.37 (1)	—	—
(e) Larger Fe(III) clusters	90	0.40 (2)	0.73 (2)	0.48 (2)	—	—
n = 40	4.1	0.50	—	0.50 (1)	370 (15)	—
n = 150 + 4[b]	4.1	0.50 (2)	—	0.50 (1)	460 (10)	—
n = 480	4.1	0.50 (2)	—	0.50 (1)	460 (2)	—

[a] LW, Full linewidth at half-maximum; QS, quadrupole splitting; IS, isomer shift; H_{eff}, effective magnetic field; T_r, relaxation time. The numbers in parentheses give the error on the last digits.
[b] $150^{56}Fe + 4^{57}Fe$. Data from Ref. *57*.

with earlier results (*61*); (2) the percentage of Fe(III) in solitary positions decreases with increasing time, increasing pH (at constant time), and increasing numbers of added iron atoms; (3) the percentage of Fe(III) in clusters increases with time, with pH, and with Fe atoms/

TABLE V

EFFECT OF TIME ON DISTRIBUTION OF IRON SPECIES MEASURED BY MÖSSBAUER SPECTROSCOPY AFTER AEROBIC ADDITION OF FOUR ^{57}Fe(II) ATOMS/APOFERRITIN MOLECULE AT VARIOUS pH VALUES

		Fe(III)						Fe(II)	
		Solitary		Dimers		Clusters			
pH	t_f[a]	%	Atoms/mol	%	Atoms/mol	%	Atoms/mol	%	Atoms/mol
5.6	17 min	60	2.4	—	—	28	1.1	12	0.5
5.6	3 hr	40	1.6	—	—	53	2.1	7	0.3
6.25	3 min	65	2.6	10	0.4	20	0.8	5	0.2
6.25	24 hr	30	1.2	2	0.08	67	2.7	1	0.02
6.4	3 min	65	2.6	12	0.5	23	0.9	—	—
6.4	20 min	63	2.5	6	0.2	31	1.2	—	—
6.4	2 hr	50	2.0	6	0.2	44	1.8	—	—
7.0	1 min	50	2.0	28	1.1	22	0.9	—	—
7.0	3 min	45	1.8	17	0.7	40	1.6	—	—

[a] t_f, Time of freezing after addition of four ^{57}Fe(II) atoms.

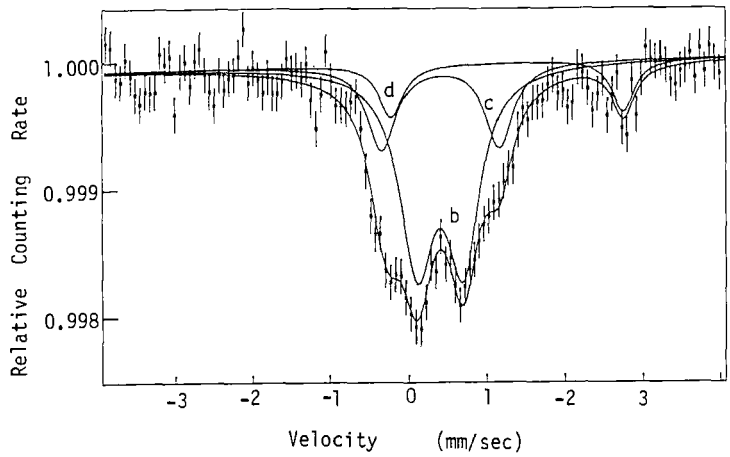

FIG. 4. A 90 K Mössbauer spectrum on an extended velocity scale of apoferritin loaded in air at pH 6.25 with four $^{57}Fe(II)$ and frozen at 3 min. The computer fit resolves the spectrum into three doublets: b, due to small clusters; c, due to oxo-bridged Fe(III) dimers; and d, due to Fe(II). Doublet d represents only 5% of the total iron. Reproduced from Ref. *69*.

molecule; (4) the percentage of Fe(III) in dimers increases with pH, decreases with time, and first increases and then declines as more Fe atoms are added; and (5) the percentage of $^{57}Fe(III)$ in clusters (at 3 min) is greatly increased when Fe is added to molecules containing a small iron core (150 ^{56}Fe) as compared to the same amount of Fe added to apoferritin. The results collectively indicate a flow of iron from solitary sites and dimers to clusters. Clusters may form around dimers, but clearly there must be movement of Fe(III) from its isolated sites to explain the results. Such migration has also been suggested by EPR experiments (*62*) and UV-difference spectroscopy (*51*). Of the above observations, the fifth is consistent with the proposal made previously (*15, 52*) that Fe(II) can bypass oxidation sites on the protein and become oxidized on the iron core. The nonintegral numbers of Fe atoms/molecule shown in Tables III and V imply a nonrandom distribution of the various Fe species even when only four Fe atoms/molecule had been added, as had been shown by analytical ultracentrifugation in ferritin reconstituted to 2000 Fe atoms/molecule (*15*). This is important to remember when interpreting the effects of iron additions: the results represent averages, possibly over wide rather than narrow ranges of iron compositions. Distributions of Fe atoms/molecule may also be affected by isoferritin composition as well as by chemical or physical factors.

Most of the reconstitution studies so far described have been done on horse spleen ferritin, a mixture of isoferritins with a range of subunit compositions, although of low average H subunit content. Recombinant human and rat ferritins containing only H or L chains (or their variants) have now been overexpressed in *E. coli* (*63–65*). Iron uptake studies with these homopolymers have not materially altered the picture of iron core formation obtained with native ferritins containing H and L chain mixtures (85% L chain in horse spleen ferritin), but differences in behavior of the two chains are shown. Core reconstitution in human H chain homopolymer initially proceeds much faster than in human liver ferritin (two to three H chains/molecule on average) or in human L chain homopolymer, but once a core is present (~1000 Fe atoms), further iron additions proceed at similar rates in all three ferritins (*63, 65*). Although rapid Fe(II) oxidation occurs on the ferroxidase centers that have been found exclusively within H chains (*16*), nevertheless iron cores do form slowly within L chain homopolymers or in H chain homopolymers in which ferroxidase centers have been inactivated (*16, 65*). In all three cases the product is ferrihydrite (*44*). Thus ferritins rich in H chains may be found in tissues in which rapid removal of iron is required. (For further discussion on molecular iron uptake mechanisms, see Section IV.)

In contrast to ferritin, very little work has been done on the reconstitution of BFR cores, other than the experiments mentioned above that showed that, in the absence of phosphate, crystalline ferrihydrite formed inside the protein shell. The intermediate stages in this process are unknown, but the sigmoid iron uptake behavior (*25*) suggests there could be a similar succession of events: oxidation and nucleation on the protein shell followed by direct oxidation on the core. The influence of the heme, if any, on BFR iron core formation also awaits investigation. As mentioned above, the presence of the iron core influences the heme redox potential, but it is not known whether the presence of heme influences the redox potential of the nonheme iron.

D. Sequestration of Fe(II) in Apoferritin

It has been suggested that ferritin can sequester relatively large amounts of Fe(II) in excess of the Fe(II) that can be bound to the Fe(III) core surface as already described (*66, 67*). Thus in some experiments, when 480 Fe(II) atoms/molecule were added (as 20 m*M* $FeSO_4$) to apoferritin at pH 7.0, a fraction of the Fe(II) became inaccessible to chelation by *o*-phenanthroline (*66, 67*). In other comparable experiments, the added Fe(II) was all chelatable by both bipyridine (*56, 68,*

69) and *o*-phenanthroline (*69*), including the fraction of Fe(II) judged to be bound to apoferritin from its Mössbauer spectral parameters (*57*). Binding experiments carried out by flow dialysis, ultrafiltration, or anaerobic gel filtration showed that, although at pH 10.0 about 80 Fe(II) atoms were bound, in the pH range 6.0–7.5 apoferritin molecules bound only 8.0 ± 0.5 atoms (*56*). Hence the sequestration by apoferritin (lacking iron core) of large amounts of Fe(II) in an inaccessible form remains controversial. About 80% of the Fe(II) produced *in situ* by reduction of holoferritin (and also holobacterioferritin) was retained during anaerobic gel filtration (*36*). This Fe(II) may have been in the form of a hydroxide complex although it was also removable by bipyridine (*56*). Holoferritin [2000 Fe(III)/molecule] was able to bind an additional 70 Fe(II) at pH 7.5 or about 300 Fe(II) at pH 10 (*56*).

There may be cellular conditions under which Fe(II) binding becomes significant, but the highly conserved nature of ligands associated with the ferroxidase center seems to emphasize the importance of oxidative iron storage mechanisms.

E. Reduction and Mobilization of Iron

Not only are iron, phosphate, and water able to penetrate the protein shell in both ferritin and BFR, but there is a considerable body of evidence that small reductants and small chelators, which are instrumental in removing iron, do so by interacting directly with the iron core in ferritin and must therefore gain access to the cavity (*61, 70–72*). One of the most interesting recent papers in ferritin and BFR biochemistry has provided data showing that reductant entry into the interior is not an essential step in iron release: core reduction in both horse spleen ferritin and the BFR of *A. vinelandii* can be effected both by dihydroflavodoxin and, more slowly, by reduced ferredoxins (*68*). With BFR, core reduction occurred without heme reduction, consistent with the lower redox potential of the latter. Core iron was also reduced in BFR that had been treated with methyl ethyl ketone at pH 2.0 to remove the protoporphyrin. Oxidation of Fe(II) bound to both ferritin and BFR was also brought about by proteins, namely, cytochrome *c'*, plastocyanin, and stellacyanin (*68*). The holoferritin was first incubated with excess Fe(II) and then subjected to Sephadex G-25 chromatography to remove unbound ferrous iron. From these experiments a question arises: How do electrons reach the core from large external redox agents (or vice versa)? Two possibilities were suggested. One is long-distance electron tunneling through the protein shell, the second

is a mediation of reduction by Fe^{2+} ions shuttling between core and protein. These possibilities are referred to later (Section IV,D). The experiments raise the interesting questions of whether redox protein partners are implicated in iron release *in vivo*.

III. The Protein Shells

A. Amino Acid Sequences

1. Ferritins

Mammalian ferritins consist of mixtures of two different polypeptide chains, known as H and L (*12, 13, 53, 61, 63, 65, 73*). Each tissue contains molecules with a range of H and L compositions, but, although H : L ratios are sensitive to tissue iron loading [which usually causes a relative increase in L subunits (*13*)], heart and brain (and also red cell) ferritin are generally H rich, and liver and spleen ferritins are generally L rich (*73*). Multiple copies of both H and L ferritin genes are found (*74–78*), many of which represent unprocessed pseudogenes (*22, 79–81*), but there is evidence for polymorphism within each class in some animals (*82*). Table VI shows amino acid sequences of H and L chains of human and rat, the H chain of chicken red cells, the L chain of horse ferritin, three sequences obtained for ferritins from *Rana catesbiana* tadpole reticulocytes (designated H, M (or H'), and L), and two for an invertebrate ferritin, *Schistosoma mansoni*. In human, rat and horse the L chains show overall 80% identity in amino acid sequence; the H chains of human, rat, and chicken show 90% identity, but only 50% of the amino acids are shared by all six ferritins. The frog and trematode ferritins resemble the H chains more closely than they do L chains, suggesting that H chains may have been developed earlier in evolution. H chains contain short extensions at N- and C-termini, compared with L chains (respective M_r values of about 21,000 and 20,000). On the other hand, L chains of rat [and also mouse (*83*)] contain an eight-residue insertion compared with the other species.

Partial sequence data for pea seed ferritin (J. F. Briat, personal communication) show regions of similarity to those of animals, but pea seed ferritin also has an N-terminal extension, unlike the N-termini of other ferritins (*84*). On SDS–PAGE, phytoferritin gives two bands, the smaller of which (M_r 26,500) is thought to have arisen from the larger (M_r 28,000), as a result of cleavage of an N-terminal peptide by hydroxyl radicals produced by iron-catalyzed Fenton reactions (*84*).

TABLE VI

Amino Acid Sequences of Some Ferritins[a]

														←														A-Helix													→	
							5					10					15					20					25					30					35					40	
1	HuLi-H		T	T	A	S	T	S	Q	V	R	Q	N	Y	H	Q	D	S	E	A	A	I	N	R	Q	I	N	L	E	L	Y	A	S	Y	V	Y	L	S	M	S	Y	Y	1
2	RaLi-H		T	T	A	S	P	S	Q	V	R	Q	N	Y	H	Q	D	S	E	A	A	I	N	R	Q	I	N	L	E	L	Y	A	S	Y	V	Y	L	S	M	S	C	Y	2
3	ChRC-H		M	A	T	P	P	S	Q	V	R	Q	N	Y	H	Q	D	C	E	A	A	I	N	R	Q	I	N	L	E	L	Y	A	S	Y	V	Y	L	S	M	S	Y	Y	3
4	TdRC-H					M	D	S	Q	V	R	Q	N	F	H	R	D	C	E	A	A	I	N	R	M	V	N	M	E	L	Y	A	S	Y	T	Y	L	S	M	A	F	Y	4
5	TdRC-M					M	V	S	Q	V	R	Q	N	Y	H	S	D	C	E	A	A	V	N	R	M	L	N	L	E	L	Y	A	S	Y	T	Y	S	S	M	Y	A	F	5
6	TdRC-L					M	E	S	Q	V	R	Q	N	F	H	Q	D	C	E	A	G	L	N	R	T	V	N	L	K	F	H	S	S	Y	V	Y	L	S	M	A	S	Y	6
7	S.ma-1						M	S	L	C	R	Q	N	Y	H	E	E	C	E	A	G	V	N	K	Q	I	N	M	E	L	Y	A	S	Y	V	Y	M	T	M	A	F	H	7
8	S.ma-2	R	K	T	M	S	S	S	R	A	R	Q	S	F	A	T	E	C	E	N	A	I	N	K	Q	I	V	E	L	Q	A	A	Y	D	Y	M	A	I	I	T	Y	F	8
9	HuLi-L						S	S	Q	I	R	Q	N	Y	S	T	D	V	E	A	A	V	N	S	L	V	N	L	Y	L	Q	A	S	Y	T	Y	L	S	L	G	F	Y	9
10	RaLi-L						T	S	Q	I	R	Q	N	Y	S	T	E	V	E	A	A	V	N	R	L	V	N	L	H	L	R	A	S	Y	T	Y	L	S	L	G	F	F	10
11	HoSp-L						S	S	Q	I	R	Q	N	Y	S	T	E	V	E	A	A	V	N	R	L	V	N	L	Y	L	R	A	S	Y	T	Y	L	S	L	G	F	Y	11

									←															B-Helix														→	(---------				
						45					50					55					60					65					70					75					80	
1	HuLi-H	F	D	R	D	D	V	A	L	K	N	F	A	K	Y	F	L	H	Q	S	H	E	E	R	E	H	A	E	K	L	M	K	L	Q	N	Q	R	G	G	R	I	1
2	RaLi-H	F	D	R	D	D	V	A	L	K	N	F	A	K	Y	F	L	H	Q	S	H	E	E	R	E	H	A	E	K	L	M	K	L	Q	N	Q	R	G	G	R	I	2
3	ChRC-H	F	D	R	D	D	V	A	L	K	N	F	A	K	Y	F	L	H	Q	S	H	E	E	R	E	H	A	E	K	L	M	K	L	Q	N	Q	R	G	G	R	I	3
4	TdRC-H	F	D	R	D	D	I	A	L	H	N	V	A	K	F	F	K	E	Q	S	H	E	E	R	E	H	A	E	K	L	M	K	D	Q	N	K	R	G	G	R	I	4
5	TdRC-M	F	D	R	D	D	V	A	L	H	N	V	A	E	F	F	K	E	H	S	H	E	E	R	E	H	A	E	K	F	M	K	Y	Q	N	K	R	G	G	R	V	5
6	TdRC-L	F	N	R	D	D	V	A	L	S	N	F	A	K	F	F	R	E	R	S	E	E	E	K	E	H	A	E	K	L	I	E	Y	Q	N	Q	R	G	G	R	V	6
7	S.ma-1	F	N	R	D	D	V	A	L	N	G	F	Y	K	F	F	L	N	E	S	E	E	E	R	Q	H	A	I	K	L	M	T	Y	Q	N	M	R	G	G	R	I	7
8	S.ma-2	F	D	R	D	D	V	S	F	P	K	A	A	E	F	F	R	K	A	S	H	E	E	R	E	H	A	E	K	L	A	K	Y	Q	N	K	R	V	G	R	V	8
9	HuLi-L	F	D	R	D	D	V	A	L	E	G	V	S	H	F	F	R	E	L	A	E	E	K	R	E	G	Y	E	R	L	L	K	M	Q	N	Q	R	G	G	R	A	9
10	RaLi-L	F	D	R	D	D	V	A	L	E	G	V	G	H	F	F	R	E	L	A	E	E	K	R	E	G	A	E	R	L	L	K	L	Q	N	E	R	G	G	R	A	10
11	HoSp-L	F	D	R	D	D	V	A	L	E	G	V	C	H	F	F	R	E	L	A	E	E	K	R	E	G	A	E	R	L	L	K	M	Q	N	Q	R	G	G	R	A	11

		------						Loop							------>	←													C-Helix												—	
						85					90					95					100					105					110					115					120	
1	HuLi-H	F	L	Q	D	I	K	K	P	D	C	D	D	W	E	S	G	L	N	A	M	E	C	A	L	H	L	E	K	N	V	N	Q	S	L	L	E	L	H	K	L	1
2	RaLi-H	F	L	Q	D	I	K	K	P	D	R	D	D	W	G	S	G	L	N	A	M	R	C	A	L	H	L	E	K	S	V	N	Q	S	L	L	E	L	H	K	L	2
3	ChRC-H	F	L	Q	D	I	K	K	P	D	R	D	D	W	E	N	G	L	T	A	M	E	C	A	L	H	L	E	K	N	V	N	Q	S	L	L	E	L	H	K	L	3
4	TdRC-H	V	L	Q	D	V	K	K	P	E	R	D	E	W	G	N	T	L	E	A	M	Q	A	A	L	Q	L	E	K	T	V	N	Q	A	L	L	D	L	H	K	V	4
5	TdRC-M	V	L	Q	D	I	K	K	P	E	R	D	E	W	G	N	T	L	E	A	M	Q	A	A	L	Q	L	E	K	T	V	N	Q	A	L	L	D	L	H	K	L	5
6	TdRC-L	F	L	Q	S	V	E	K	P	E	R	D	D	W	A	N	G	L	E	A	L	Q	T	A	L	K	L	Q	K	S	V	N	Q	A	L	L	D	L	H	A	V	6
7	S.ma-I	V	L	Q	D	I	S	A	P	P	Q	S	L	W	N	S	G	L	H	A	M	Q	D	A	L	D	L	E	K	K	V	N	Q	S	L	M	E	L	V	A	V	7
8	S.ma-2	Q	Y	S	D	I	K	C	P	T	K	T	E	F	S	S	L	E	D	A	M	N	T	A	L	G	M	E	K	A	V	S	K	S	L	L	E	L	H	E	V	8
9	HuLi-L	L	F	Q	D	I	K	K	P	A	E	D	E	W	G	K	T	P	D	A	M	K	A	A	M	A	L	E	K	K	L	N	Q	A	L	L	D	L	H	A	L	9
10	RaLi-L	L	F	Q	D	V	Q	K	P	S	Q	D	E	W	G	K	T	L	E	A	M	E	A	A	L	A	L	E	K	N	L	N	Q	A	L	L	D	L	H	A	L	10
11	HoSp-L	L	F	Q	D	L	Q	K	P	S	Q	D	E	W	G	T	T	L	D	A	M	K	A	A	I	V	L	E	K	S	L	N	Q	A	L	L	D	L	H	A	L	11

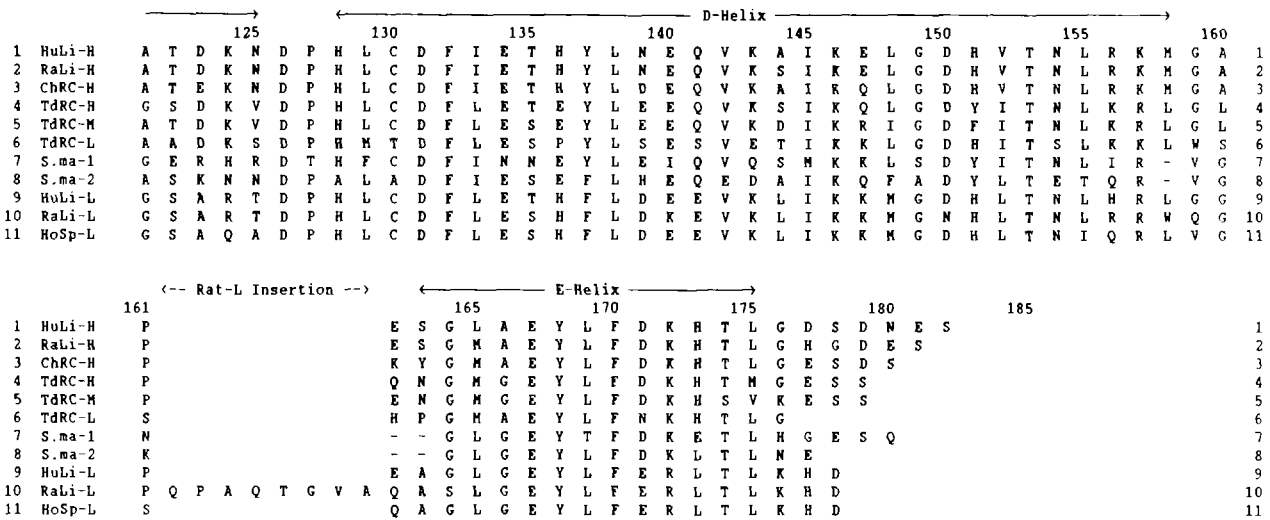

[a] Key: 1, human liver H chain (*74*); 2, rat liver H chain (*22*); 3, chicken red cells (*75*); 4, 5, 6, bullfrog tadpole red cells (*18*); 7, 8, *Schistosoma mansoni* sequences 1 and 2 (*76*); 9, human liver L chain (*74*); 10, rat liver L chain (*77*); 11, horse spleen L chain (*78*). Sequences use human H chain numbering. Secondary structure elements are indicated.

2. *Bacterioferritins*

The complete amino acid (gene-derived) sequence for the BFR of *E. coli* (*85*) is shown in Table VII together with partial sequences of BFRs from *A. vinelandii* (*86*) and *Nitrobacter winogradskyi* (*87*). These form a group of related proteins, but one that has no significant homology with the ferritins of Table VI. Thus the BFRs form a distinct class of molecules. The subunit size of *E. coli* BFR (158 amino acids, M_r 18,495) is rather less than those of the ferritins. Both *A. vinelandii* and *N. winogradskyi* BFRs can give two apparent subunit bands on electrophoresis in denaturing gels (*86–88*), but these are dependent on thiol treatment or heme content, respectively, and may not represent isobacterioferritins. Microheterogeneity in partial sequences of the BFR of *P. aeruginosa* has been observed (G. R. Moore, personal communication), but the significance of this is uncertain.

TABLE VII

AMINO ACID SEQUENCE DATA FOR THREE BACTERIOFERRITINS[a]

Bacterium	Amino acid sequence
	1 10 20 30
Escherichia coli[b]	M K G D T K V I N Y L N K L L G N E L V A I N Q Y F L H A R
Azotobacter vinelandii[c]	M K G D K I V I Q H L N K I L G N E L I A I N Q Y F L H A R
Nitrobacter winogradskyi[d]	M K G D P K V I D Y L N K A L R H E L T A I N Q Y W L H Y R
	40 50 60
Escherichia coli	M F K N W G L K R L N D V E Y H E S I D E M K H A D R Y I E
Azotobacter vinelandii	M Y E D W G L E K L G K H E Y H E S I D E M K H A D K L I (K)
Nitrobacter winogradskyi	L L D N W G I K D L A K K W R A E S I E
	70 80 90
Escherichia coli	R I L F L E G L P N L Q D L G K L N I G E D V E E M L R S D
Azotobacter vinelandii	R I L F L E X (L) (P) N
	100 110 120
Escherichia coli	L A L E L D G A K N L R E A I G Y A D S V H D Y V S R D M M
	130 140 150
Escherichia coli	I E I L R D E E G H I D W L E T E L D L I Q K M G L Q N Y L
	158
Escherichia coli	Q A Q I R E E G

[a] Helical regions predicted from the sequence of *E. coli* BFR (*85*) are approximately 6–34, 36–65, 78–105, 115–143, and 150–157, and a possible four-helix bundle motif is shown in Fig. 10.

[b] Data from Ref. *85*.

[c] Data from Ref. *86*.

[d] Data from Ref. *87*.

B. X-Ray Crystallographic Data and Shell Symmetry

1. Ferritin and Apoferritin

Horse spleen apoferritin (about 85% L chain) has been crystallized in two forms: face-centered cubic, a = 184 Å, space group F432, with four molecules in the unit cell (*89*); and tetragonal, $a = b$ = 147 Å, c = 154.5 Å, space group $P42_12$ (pseudo-body-centered cubic), with two molecules in the unit cell (*90*). Ferritin (or apoferritin/ferritin mixtures) gives isomorphous crystals in both crystalline forms, demonstrating that the presence of ferrihydrite does not affect molecular packing in the crystals. The single-crystal X-ray diffraction patterns show marked intensity differences only at very low angles, but, at very high angles, powder lines due to disoriented ferrihydrite appear (*91*). Hence, not only is the structure of the protein shell virtually unaffected by the presence of the iron core, but the ferrihydrite atomic structure is not specifically related to that of the protein.

A third, orthorhombic, crystalline form has been obtained for horse spleen ferritin, but not apoferritin. It has a = 130 Å, b = 130 Å, c = 184 Å, and space group $P22_12_1$, and is closely related to the face-centered cubic form, with a and b lying along face diagonals of the cube (92). All three crystal forms have been obtained by precipitation with $CdSO_4$ under slightly different conditions. Rat liver, mouse liver (*93*), recombinant rat L ferritin (*64*), and recombinant human H ferritin all give face-centered cubic crystals essentially isomorphous with those of horse spleen ferritin (*94*). The first three of these were grown in the presence of $CdSO_4$.

Very low-angle X-ray data (26 Å resolution) of horse spleen apoferritin fit approximately the Fourier transform of a uniform spherical shell with inner and outer diameters of 76 and 122 Å (*92, 95*). Low-angle difference X-ray data for ferritin and apoferritin indicate iron cores of high scattering power that are approximately spherical (d = 78 Å) (*92*). Cubic crystal point symmetry shows that ferritin molecules are composed of 24 structurally equivalent subunits related by 432 symmetry, there being one polypeptide chain per asymmetric unit. In mixed H and L chain copolymers, the apparent structural equivalence must be statistical, although very similar chain conformations are expected.

2. Bacterioferritin

Native BFR (ferriheme) from *E. coli* has given several crystalline forms: monoclinic, two closely related orthorhombic, tetragonal, and

cubic (*96, 97*). The orthorhombic crystal forms with a = 128.7 Å, b = 197.1 Å, and c = 202.8 Å and a = 130.8 Å, b = 191.6 Å, and c = 201.1 Å, both of space group $C222_1$, are closely related to an orthorhombic crystal form of the BFR of *A. vinelandii* with a = 120.9 Å, b = 201.1 Å, and c = 216.8 Å, also of space group $C222_1$, suggesting the molecules are of similar packing diameters (*96, 97*). The tetragonal form with $a = b$ = 210.6 Å, c = 145.0 Å, and space group $P4_22_12$ can be transformed, by soaking the crystals in tetrakisacetoxymercurimethane, into a body-centered cubic modification with a = 146.9 Å, space group I432, and two molecules in the unit cell (*96, 97*). Note the similarity in these cell dimensions and those of the tetragonal (pseudocubic) form of horse spleen apoferritin, again suggesting similar molecular diameters. This similarity is confirmed by analysis of low-angle diffraction data that can be fitted approximately by the Fourier transform of a uniform hollow shell with external and internal diameters, respectively, of 120.6 and 60.8 Å (*95*), close to the dimensions of horse spleen apoferritin, although in the latter the fit to a uniform hollow sphere is more exact. A cubic form of *E. coli* BFR has also been grown from CsCl solution (a = 150.8 Å; I432) (*24, 97*).

Isomorphous tetragonal crystals are obtained for *E. coli* BFR, whether loaded or poor in nonheme iron (*97*), with marked intensity differences only at very low angles. Thus in BFR, as in the case of ferritin, the iron core mineral has little affect on the structure of the protein shell and is not structurally related to it. In this study the iron-loaded molecules were shown to contain ferrihydrite (*47*). The *E. coli* BFR with a wide range of estimated heme contents (0.5–0.01 per subunit) also gave isomorphous tetragonal crystals, as did a BFR-λ fusion protein (*98*) containing a C-terminal extension of 14 residues (18 residues from the λ protein attached after residue number 154 of BFR). The extensions probably lie within the shell, and, if so, about 60% of the cavity would be occupied by protein. This BFR takes up little or no nonheme iron and its heme content is also low (*99*).

In the above crystals, BFR molecules contained ferriheme. The *E. coli* BFR crystallized under anaerobic conditions with heme in the ferro form gave tetragonal crystals of slightly different dimensions, $a = b$ = 209 Å and c = 147 Å, space group $P4_22_12$.

C. Subunit Conformation and Quaternary Structure

1. Ferritins

The three-dimensional structures of horse spleen apoferritin (85% L, 15% H subunit) (*11*), rat liver ferritin (66% L, 34% H subunit) (*94*),

recombinant rat L ferritin (rLF; 100% L) (*64, 94*), and recombinant human H ferritin (rHF; 10% H) (*69, 94, 115*) as well as several genetically engineered variants of the latter (*94, 100*) have all been determined at high resolution. These ferritins have almost the same conformations and quaternary structures, most of the backbone atoms being superposable within ±1.0 Å (Fig. 5). The subunit conformation is a 4-α-helix bundle composed of two antiparallel helix pairs (AB and CD). Helices in each pair are joined by a short turn, AB or CD, but between B and C there is a long connection of 17 residues spanning the length of the bundle. The bundle is capped at one end by a fifth helix, E, lying at about 60° to its axis, and at the other end (the N-terminus) there is a short, variable nonhelical stretch of 8–12 residues. At the C-terminal end there are 2–8 residues extending from the E helices. The E helices lie nearly parallel to the radius vector of the almost spherical molecule with their C-terminal ends, and their additional C-terminal residues, protruding into the molecular cavity. In the molecular structure, subunits lie in antiparallel pairs, making flat rhombs, and the whole structure, with 12 such rhombs, approximates to a rhombic dodecahedron (an archimedean solid) (*101*). The apices of the dodecahedron are truncated and the long BC connecting loops lie antiparallel on the centers of the rhomb faces, so that the overall appearance of the molecule is more nearly spherical than polyhedral. Figure 6 shows a stereo diagram of five half molecules arranged on a face center of the cubic unit cell, which displays both molecular packing within the crystal and

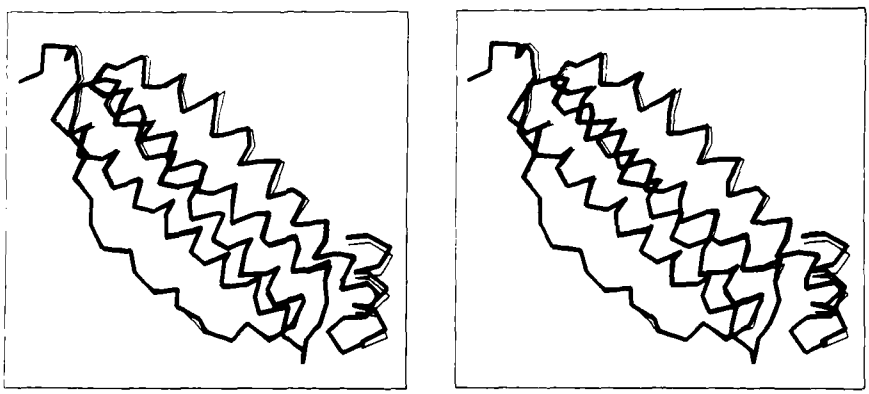

FIG. 5. Stereo α-carbon trace of a single subunit of human rHF (heavy line) superposed on that of rat rLF. There is no clear electron density for the eight residues inserted in the rat light subunit sequence in the DE turn or for the C-terminal residues that extend beyond the E helix (lower right). The inside surface of the molecule lies at the upper right and the outer surface lies at the lower left corner of the diagram.

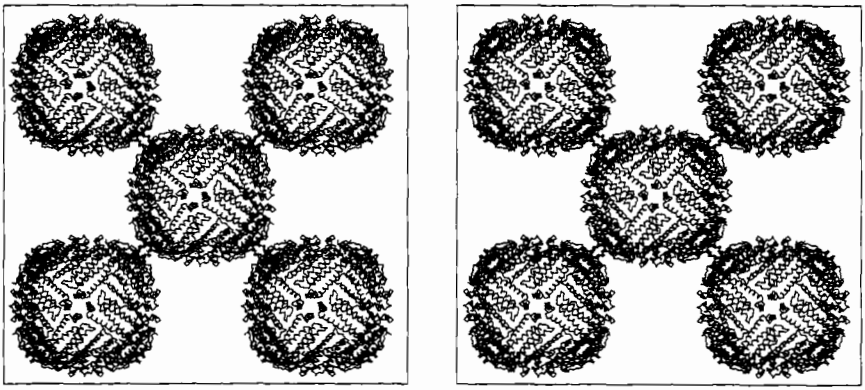

FIG. 6. Stereo diagram showing packing of molecules on a face of the face-centered cubic crystal of human rHF. For clarity, only 16 of the 24 subunits are shown. A "lid" of 8 subunits has been removed so that molecules are seen as hollow shells looking down a four-fold axis into their interiors. Subunits are drawn as α-carbon traces. Four intermolecular crystal contacts of the central molecule can be seen and a close-up of one of these is depicted in Fig. 7.

subunit packing within the molecule. Molecules are linked in the crystal through double metal ion bridges (Fig. 7). Depending on the salt from which the ferritin was crystallized, the metal ions can be Cd^{2+}, Ca^{2+}, or Tb^{3+}. The metal ions are coordinated by four aspartates and four glutamines (two of each residue from neighboring molecules). In human rHF, metal bridges were engineered by substitution of glu-

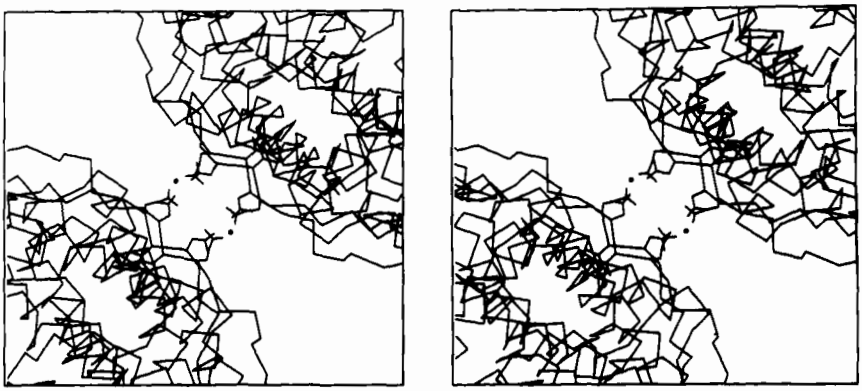

FIG. 7. Stereo view of crystal contact region in human rHF crystals. Black dots represent Ca^{2+} ions. Metal ion ligands are provided by Asp 82 and Gln 86 on the loop regions of two neighboring subunits and by the equivalent residues of the neighboring molecule. Note that Gln 86 was introduced by mutagenesis in place of Lys 86 to enable crystallization to take place by metal bridge formation (*115*).

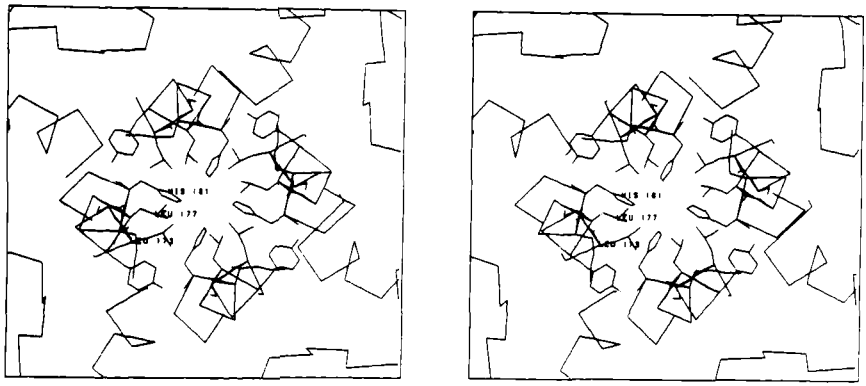

FIG. 8. Stereo view of the region around a four-fold channel in human rHF viewed from inside the cavity. The channel is surrounded by four histidines (cavity side) and eight leucines.

tamine for the lysine (sequence number 86) present in the native sequence (the first successful engineering of a crystal contact). Crystallization was effected with $CaCl_2$, rather than $CdSO_4$, however, the latter produced only amorphous precipitates. There are many intersubunit interactions within the quarternary structure giving a close-packed shell, except that at the four-fold and three-fold symmetry axes there are small pores or channels about 3 Å wide (Figs. 8 and 9). In horse spleen and rat L ferritins, the four-fold channels are hydrophobic, be-

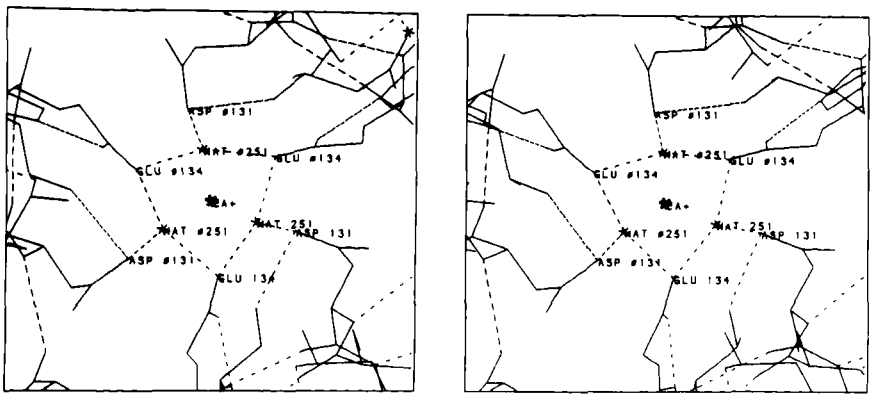

FIG. 9. Stereo diagram of the three-fold channel region of human rHF viewed from outside the molecule. Only the narrow end of the channel, toward the cavity, is shown. In the center of the channel there is a large peak of electron density presumed to represent a Ca^{2+} ion (marked here with a star). It has six oxy ligands supplied by three glutamates and three waters (hydrogen bonded to aspartates) in octahedral geometry.

ing surrounded by 12 leucines, three from each of the four adjoining subunits. These leucines lie along one edge of each of the four nearly parallel E helices that make the channel. In human H ferritin, the leucines near the C-terminal ends of the E helices (toward the inside surface of the molecule) are replaced by histidine residues (Fig. 8). Near to these histidines in the human rHF electron density map there is a peak of high density, which may represent a metal ion coordinated to them. This peak is not found in electron density maps of L ferritins. At the three-fold axes the channels are hydrophilic in character (Fig. 9). Except for variants having changes in these residues, the three aspartates (toward the inside surface) and three glutamates, which protrude into the narrowest part of the channel, are also found to bind metal ions in all the crystal structures of ferritins so far examined (*11, 53, 64, 69, 93, 94, 100*): two Cd^{2+} or two Zn^{2+} ions (coordinated by either three aspartates or three glutamates) or a single Tb^{3+} or Ca^{2+} (with all six carboxylates or with three carboxyls and three waters as ligands). Figure 9 shows a single Ca^{2+} in rHF. Each ferritin molecule has eight three-fold channels and six four-fold channels. The aspartates (residue number 131) and glutamates (residue number 134) of the three-fold channels are highly conserved in most ferritins. However, in one of the two ferritin sequences of the parasite *S. mansoni* (Table VI), glutamic acid number 134 is replaced by asparagine. This same ferritin has changes in the four-fold channel residues as well. Instead of three leucines at residue numbers 165, 169, and 173, or two leucines and one histidine, it has leucine, threonine, and glutamic acid, respectively. A considerable number of residues involved in intrachain or interchain contacts are conserved in all ferritin sequences, suggesting they are essential for subunit folding and shell assembly.

On the inside of the apoferritin shell the antiparallel B and D helices of the subunit pairs form a ridged surface partly filled by side chains and water molecules. Water molecules also cluster at the ends of helices within intersubunit contact regions. In horse spleen L ferritin, several metal-ion-binding sites have been found on the inside surface (*11, 53*); the possibility that some of these might represent iron sites leading to ferrihydrite nucleation has been referred to above and is discussed further in Section IV,C.

2. *Bacterioferritin*

In the absence of a high-resolution three-dimensional structure of a BFR, a tentative subunit conformation (Fig. 10) has been derived by secondary structure prediction from amino acid sequence data. A combined prediction based on eight different programs gave a helical dis-

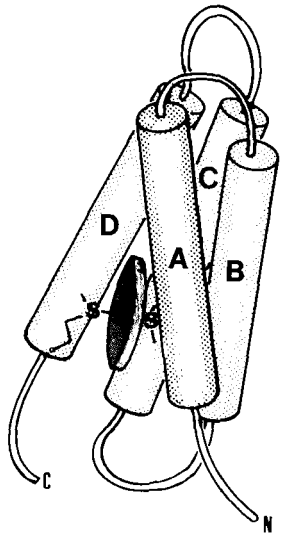

FIG. 10. Speculative model of a subunit of the BFR of *E. coli*. The conformation is a four-helix bundle as predicted from the amino acid sequence (*85*). Heme axial ligation is assumed to be bis(methionine) according to Ref. *105*. Methionines 86 and 144 are placed near the N- and C-termini, respectively of helices C and D in the model and the heme is shown attached to these methionines. The heme position differs from that in cytochrome b_{562}, in which it is linked to helices A and D (*104*).

tribution quite close to that observed by X-ray crystallography for both horse (*102*) and rat L ferritin sequences (*53*), and single predictions for both human H and L ferritins suggested a similar secondary structure (*74*). For the *E. coli* BFR sequence of Table VII, the combined prediction suggests that about 80% of the amino acids lie on four long helical regions with the possibility of a fifth short helix at the C-terminus (*85*). A four-helix bundle conformation like that of ferritin seems likely, except that the sequence is shorter and the long BC connecting loop is replaced by a turn containing only about 10 residues. This suggests that the subunit fold in BFR (Fig. 10) may resemble those of cytochromes *c'* (*103*) and b_{562} (*104*) more closely than that of ferritin (*11*). It is tempting to speculate that two four-helix bundles align antiparallel as in cytochrome *c'* (*103*) and in ferritin (*11*), and, if so, the quaternary structure of BFR may be a rhombic dodecahedron like that of ferritin (*101*). It would be of great interest if such similar structures had arisen independently in evolution from quite disparate amino acid sequences.

Based on combined EPR and magnetic circular dichroism data obtained for the BFRs of *P. aeruginosa*, *A. vinelandii*, and *E. coli*, bis-

(methionine) axial heme ligands have recently been proposed, the first time such coordination has been found in a protein (*105*). The amino acid sequence of the BFR of *E. coli* contains seven methionines at positions 1, 31, 52, 86, 119, 120, and 144. Of these, position 31 is substituted by leucine in *N. winogradskyi* BFR (*87*), so it is unlikely to be a heme ligand. In cytochrome b_{562} the axial heme iron ligands (methionine and histidine) lie close to the N- and C-termini, so that the protoporphyrin group links helices A and D at one end of the bundle (the helices are prized apart to make room for the heme ring). The conformation of cytochrome c' resembles that of b_{562} except that the heme iron has a single protein ligand, a histidine residue (*103, 104*). If the BFR subunit conformation is similar, methionines 1 and 144 may be the ligands. However, residue 1 is predicted to be in a nonhelical region and an alternative conformation is shown in Fig. 10. This has the protoporphyrin iron coordinated to methionines 86 and 144, respectively, near the N- and C-termini of helices C and D. Weak binding due to bis(methionine) may account for the relatively low and variable occupancy of heme groups. Nevertheless, the subunit conformation and quaternary structures of such BFRs are virtually identical, as judged by their X-ray diffraction patterns (*96, 97, 99*). The presence or absence of heme seems, therefore, to have little influence on the protein fold in BFR, in contrast to myoglobin, in which the secondary structure develops fully only when protoporphyrin is present (*106*).

IV. Mineralization Mechanisms in H and L Ferritins

A. Localization of the Ferroxidase Center on H Chains

The presence of ferroxidase centers only on H chains was inferred from comparisons of iron uptake properties of human rHF and rLF (*16, 63, 65*) and rat rLF (*64*) as well as of several native ferritins of different subunit compositions (*107*). Such a center was not identified, however, until a new metal site, not present in any L subunit structure, was discovered by X-ray crystallography of rHF (*94, 115*), and its associated ferroxidase activity was proved by means of site-directed mutagenesis, which eliminated this activity (*16*). Figure 11 shows the positions of the metal center within the subunit (probably occupied by Ca^{2+} in crystals grown from $CaCl_2$) and Fig. 12 gives a schematic drawing of the site and its immediate surroundings, as well as the equivalent region of the L subunit. In the latter the metal center is replaced by a salt bridge. In human H ferritin the metal ligands are

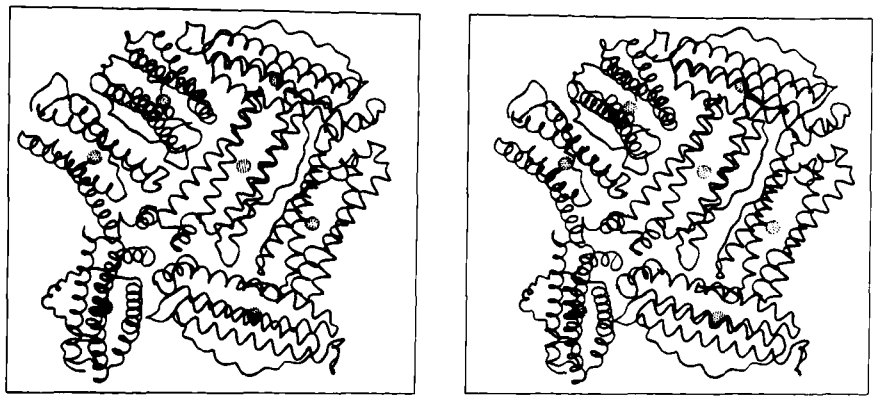

FIG. 11. Stereo ribbon diagram of part of the outer surface of a molecule of human rHF. The positions of ferroxidase centers are shown as spheres. Note that they occupy roughly central positions within the subunit.

Glu 27, Glu 62, and His 65. In human and horse L ferritin these residues are replaced, respectively, by Tyr, Lys and Gly and in rat L ferritin, by His, Lys, and Gly. Examination of the sequences of ferritins given in Table VI shows that residues Glu 27, Glu 62, His 65, and the nearby Glu 107 and Gln 141 that make hydrogen bonds to a metal-coordinated water are conserved in H chains of human, rat, and chicken. They are also found in tadpole H and M subunits and the two sequences of *Schistosoma* ferritin (*76*) (which were designated H on the basis of their greater similarity to H than to L chains). Thus the ferroxidase center seems to be a property of primitive H chains as well as of mammalian H ferritins. The tadpole L chain (*18*) does not have these residues conserved, although it has 61% identity with human H chain and only 49% with human L and is also more similar to rat H chains (63%) than L chain (49%). It has residues Lys 27, Gln 107, and Ser 141 in place of Glu 27, Glu 107, and Gln 141 and hence would not be expected to show activity.

The ferroxidase metal site has distorted tetrahedral geometry. The two carboxyls supply only two oxy ligands; a third ligand is Nδ1 of His 65 and a fourth is a peak attributed to water. Additional water molecules may be present in the coordination shell, but there are no other clearly defined peaks of electron density. The geometry of the metal site in five human rHF variants (four of them carrying sequence changes in the three-fold channels) is somewhat variable, suggesting that it is not rigidly defined by the protein (*115*). This flexibility, together with the rather limited coordination supplied by protein side

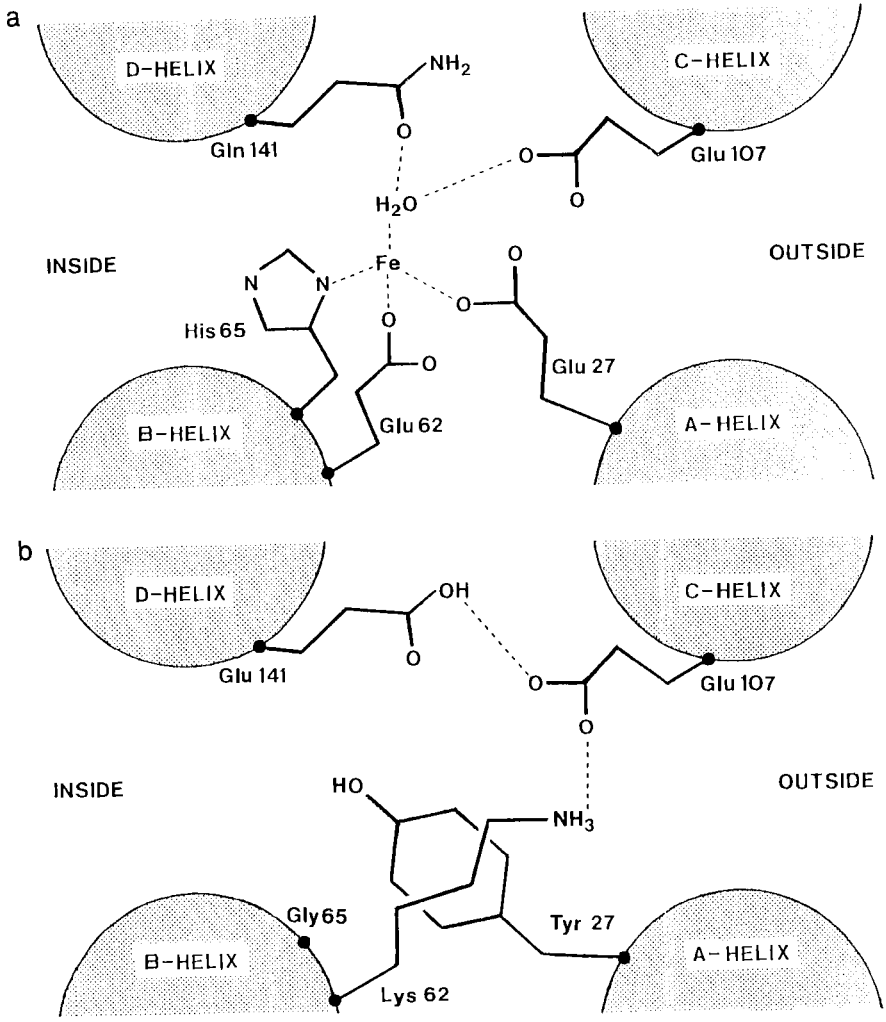

FIG. 12. Schematic diagram of the ferroxidase center of human rHF (a), and the equivalent region of horse light-chain ferritin (b) showing the ferroxidase site replaced by a salt bridge.

chains, may be a functionally important feature, designed to allow the ferric iron to leave the ferroxidase center after oxidation.

Can any of the spectroscopically characterized Fe(III) atoms be identified with iron at the ferroxidase center? EPR (*56, 60*), Mössbauer (*57*), and UV-difference (*51*) spectroscopy suggest that the first iron oxidized is at isolated sites, but that the Fe(III) then migrates to clus-

ter sites. It would seem reasonable to postulate that this initial, solitary Fe(III) lies on H chain ferroxidase centers. Evidence for this hypothesis is the finding that the absorption due to the initial Fe(III)–apoferritin complex is not observed in a variant bearing the sequence changes Glu 62 → Lys and His 65 → Gly. Nevertheless, it is possible that the Fe(III) had already moved before the observations were made or that the solitary iron represents a mixture of sites. Horse spleen ferritin contains an average of about three H chains per molecule, but binding and EPR measurements suggest about 8 Fe^{2+} or 7–12 Fe^{3+} are bound (*56, 60*). Under anaerobic conditions, Fe^{2+} may bind at other sites, possibly in the three-fold channels, instead of, or as well as, at the ferroxidase centers.

B. How Does Iron Enter the Ferritin Molecule?

Two types of intersubunit channels have already been identified. The predominantly hydrophobic four-fold channels may be expected to present an energy barrier to charged iron species, unless they are shielded, e.g., by chelating molecules. Changing His 173 of the H chain four-fold channels to leucine (as in L chains) did not reduce the rate of iron uptake (*63*). The three-fold channels, which are known to bind metal ions, have been postulated as the likely entry ports for Fe^{2+} (*11, 61, 109, 110*). However, the glutamates and aspartates of the three-fold channel are not essential for iron entry: when these were changed to histidines core formation still occurred (*109*). The reduced rate of core deposition observed, however, could have meant that the histidine impeded entry. Little or no Ca^{2+} is bound in the three-fold channels that have one of the following changes: Asp 131 → His, Glu 134 → Ala, or Glu 134 → His (*108*). The three-fold channel region of the first of these variants is shown in Fig. 13.

An alternative route through the shell has been found in rHF. There appears to be a narrow passage (or "one-fold" channel) in the subunit leading directly to the ferroxidase center (*94, 115*). This would give a pathway of about 12 Å to this site compared with over 50 Å via the three-fold channels. However, the route or routes by which Fe(II) reaches the ferroxidase center remains uncertain. In L ferritins, in which the "one-fold" channel is blocked, entry into the cavity may be via the three-fold channels.

C. Where Do Dimers and Larger Clusters Form?

A means of shepherding Fe^{3+} ions formed at the ferroxidase center into the cavity is suggested by crystallographic analysis of the Tb^{3+}

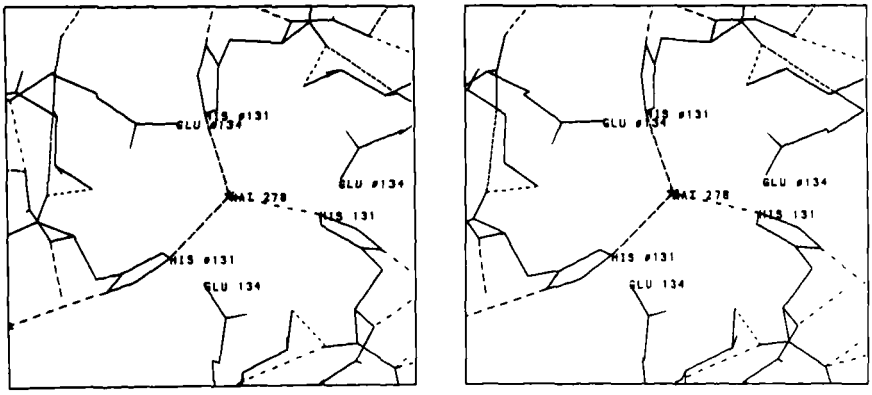

FIG. 13. Stereo view of the inner, narrow part of the three-fold channel region of a variant of human rHF in which Asp 131 has been replaced by His. The large peak of electron density seen in the center three-fold channels of wild type rHF (Fig. 9) is absent. Instead, a low-density peak that may represent a water molecule H-bonded to three His 131 molecules is found and is shown here. Note that because of differences in ligand preferences, the absence of a Ca^{2+} site in these channels does not necessarily mean that Fe^{2+} cannot bind here.

derivative of rHF (*115*). Figure 14 shows electron density due to Tb^{3+} at this center. There seem to be three neighboring Tb^{3+} sites: two within an elongated peak at the ferroxidase center (A and B) and the third (C) on the inside surface. Site A is the same as that thought to be the center of ferroxidase activity. Site B is about 3 Å from site A toward the cavity and it may be presumed that these represent alternative Tb^{3+} positions. The two positions of Glu 61 in Fig. 14 should be noted. Electron density for this amino acid is weak and it seems to alternate as ligand for the Tb^{3+} ions at B and C. Its movement suggests a way of moving Fe^{3+} from A to C via B. Note that site C is similar to a Tb^{3+} site previously found in horse spleen apoferritin (*53*) and that its ligands are two of the three glutamates (numbers 61, 64, and 67) previously mentioned as being conserved in almost all known ferritin sequences, including those of L subunits, and originally postulated as the nucleation site (*53*). However, if Fe^{3+} remains attached to Glu 61 after reaching the cavity, this residue is no longer available to deliver more iron. Migration could, nevertheless, be envisaged from other centers, because a single nucleus is all that is needed to drive core formation. Mutagenesis experiments are being used to attempt to define the roles of residue 61 and of 64 and 67. Preliminary work shows that changing these three glutamates to alanine markedly reduces the rate of core formation, but not to zero (*111*). In *Schistosoma* ferritin sequence 1

(Table VI), only Glu 61 is conserved, so the two neighboring glutamates may not be essential for iron storage.

There is no information on the site of formation of the Fe(III)–O–Fe(III) dimers that have been observed in rHF as well as in horse spleen ferritin (*57, 112*). This may be clarified by Mössbauer spectroscopy on ferritin variants. Possible positions are the putative nucleation center or the double Tb^{3+} site. In the latter case, either the dimers themselves must move or the iron core nucleus must incorporate iron atoms from the ferroxidase centers. Because ferrihydrite can be deposited both in rLF and in the rHF variant lacking ferroxidase activity, nucleation at this center is not possible for these molecules. Indeed, a specific center may not be required. However, electron micrographs of broken ferritin molecules suggest an attachment of ferrihydrite to the protein shell (*113*).

An alternative suggestion has been made that Fe(III) clustering starts in the three-fold channels and that the core grows from one of these positions (*114*). However, this can be ruled out, because core formation proceeds in variants in which the channel aspartates and glutamates have been changed (*109*).

The structural basis of iron storage in bacterioferritins is unknown at present, but parallel structure–function studies should eventually enormously increase our understanding of the processes by which iron can be sequestered in these molecules.

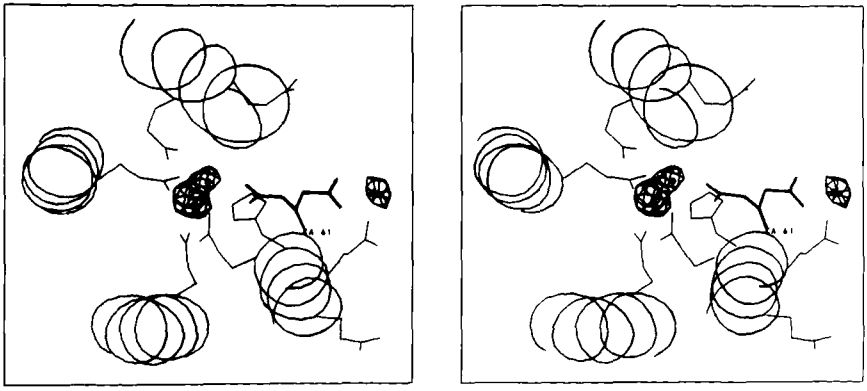

FIG. 14. Stereo view of the central part of a subunit of human rHF showing the positions of density attributed to Tb^{3+} ions in a derivative crystal. The elongated peak of high density represents two alternative Tb^{3+} positions. The lower peak (closest to histidine) coincides with the ferroxidase center. Adjacent to this is a second site close to Glu 61. Note that Glu 61 has a second (alternative) conformation in which it binds a third Tb^{3+} on the inner surface of the molecule (right-hand side). Movement of Glu 61 may facilitate movement of Tb^{3+} between B and C (*115*).

D. Reduction or Oxidation at a Distance

No mention has been made until now of the position adopted by dioxygen during ferroxidase action. This is at present unknown. It may bind directly to the Fe atom, possibly displacing water, or an outer-sphere mechanism could be envisaged.

The pathway by which electrons traverse the shell when proteins are involved in redox processes in ferritin is also unknown. It is conceivable that iron at the ferroxidase site is involved in passing electrons. It seems to be linked to the outside of the protein shell through a string of covalent and hydrogen bonds and there are also aromatic residues in its neighborhood. The involvement of an Fe^{2+}/Fe^{3+} shuttling between core and three-fold channel sites is an alternative suggestion (*56*). Tunneling of electrons through the protein without the involvement of metal ions (along E helices?) is yet another possibility. Probing these alternative routes could provide new information about ferritin and add to our understanding of electron transfer processes in proteins.

Acknowledgments

We thank the Wellcome Trust, the Science and Engineering Research Council, and the Commission for European Communities (BAP contract No. 0253UK) for support. P. J. Artymiuk acknowledges receipt of a Royal Society University Research Fellowship and G. C. Ford is a Wellcome Trust Reader. Studies on recombinant ferritins were carried out in collaboration with A. Luzzago, G. Cesareni, S. Levi, P. Arosio, C. D. Thomas, and W. V. Shaw, and Mössbauer spectroscopic studies with E. R. Bauminger and I. Nowik.

References

1. Williams, R. J. P., *FEBS Lett.* **140,** 3 (1982).
2. Williams, R. J. P., *Eur. J. Biochem.* **150,** 231 (1985).
3. Williams, R. J. P., *Biochem. Soc. Trans.* **18,** 689 (1990).
4. Williams, R. J. P., *in* "Biomineralization" (S. Mann, J. Webb, and R. J. P. Williams, eds.), p. 1. VCH Publ., Weinheim, 1989.
5. Williams, R. J. P., *Nature (London)* **343,** 213 (1990).
6. Balkwill, D., Maratea, D., and Blakemore, R. P., *J. Bacteriol.* **141,** 1399 (1980).
7. Webb, J., Macey, D. J., and Mann, S., *in* "Biomineralization" (S. Mann, J. Webb, and R. J. P. Williams, eds.), p. 345. VCH Publ., Weinheim, 1989.
8. Spiro, S., and Guest, J. R., *FEMS Microbiol. Rev.* **75,** 399 (1990).
9. Neilands, J. B., *Annu. Rev. Biochem.* **50,** 715 (1981).
10. Bagg, A., and Neilands, J. B., *Biochemistry* **26,** 5471 (1987).
11. Ford, G. C., Harrison, P. M., Rice, D. W., Smith, J. M. A., Treffry, A., White, J. L., and Yariv, J., *Philos. Trans. R. Soc. London, Ser. B* **304,** 551 (1984).
12. Theil, E. C., *Annu. Rev. Biochem.* **56,** 289 (1987).

13. Theil, E. C., *Adv. Enzymol.* **63,** 421(1990).
14. Bielig, H. J., and Bayer, E., *Naturwissenschaften* **42,** 125 (1955).
15. Macara, I. G., Hoy, T. G., and Harrison, P. M., *Biochem. J.* **126,** 343 (1972).
16. Lawson, D. M., Treffry, A., Artymiuk, P. J., Harrison, P. M., Yewdall, S. J., Luzzago, A., Cesareni, G., Levi, S., and Arosio, P., *FEBS Lett.* **254,** 207 (1989).
17. Drysdale, J. W., and Munro, H. N., *J. Biol. Chem.* **241,** 3630 (1966).
18. Dickey, L. F., Sreedharan, S., Theil, E. C., Didsbury, J. R., Wang, Y.-H., and Kaufman, R. E., *J. Biol. Chem.* **262,** 7901 (1987).
19. Mulher, E. W., Neupert, B., and Kuhn, L. C., *Cell (Cambridge, Mass.)* **58,** 373 (1989).
20. Roualt, T. A., Hentze, M. W., Wright Caughman, S., Harford, J. B., and Klausner, R. D., *Science* **241,** 1207 (1988).
21. Leibold, E. A., and Munro, H. N., *Proc. Natl. Acad. Sci. U. S. A.* **85,** 2171 (1988).
22. Murray, M. T., White, K., and Munro, H. N., *Proc. Natl. Acad. Sci. U. S. A.* **84,** 7438 (1987).
23. Farrant, J. L., *Biochim. Biophys. Acta* **13,** 569 (1954).
24. Yariv, J., Kalb, A. J., Sperling, R., Bauminger, E. R., Cohen, S. G., and Ofer, S., *Biochem. J.* **197,** 171 (1981).
25. Mann, S., Williams, J. M., Treffry, A., and Harrison, P. M., *J. Mol. Biol.* **198,** 405 (1987).
26. Mann, S., Bannister, J. V., and Williams, R. J. P., *J. Mol. Biol.* **188,** 225(1986).
27. Towe, K. M., and Bradley, W. F., *J. Colloid Interface Sci.* **24,** 384 (1967).
28. Harrison, P. M., Fischbach, F. A., Hoy, T. G., and Haggis, G. H., *Nature (London)* **216,** 1188 (1967).
29. Harrison, P. M., and Hoy, T. G., *in* "Inorganic Biochemistry" (G. L. Eichhorn, ed.), p. 253. Elsevier, New York, 1973.
30. St. Pierre, T. G., Bell, S. H., Dickson, D. P. E., Mann, S., Webb, J., Moore, G. R., and Williams, R. J., *Biochim. Biophys. Acta* **870,** 127 (1986).
31. Williams, J. M., Danson, D. P., and Janot, C., *Phys. Med. Biol.* **23,** 835 (1978).
32. Chadwick, J. C., Jones, D. H., Thomas, M. F., and Devenish, M., *Hyperfine Interact.* **28,** 537 (1968).
33. Bauminger, E. R., Cohen, S. G., Dickson, D. P. E., Levy, A., Ofer, S., and Yariv, J., *Biochim. Biophys. Acta.* **623,** 237 (1980).
34. Watt, G. D., Frankel, R. B., Papaefthymiou, G. C., Spartalian, K., and Stiefel, E. I., *Biochemistry* **25,** 4330 (1986).
35. Andrews, S. C., Brady, M. C., Treffry, A., Williams, J. M., Mann, S., Cleton, M. I., de Bruijn, W., and Harrison, P. M., *Biol. Met.* **1,** 33 (1988).
36. Watt, G. P., Frankel, R. B., and Papaefthymiou, G. C., *Proc. Natl. Acad. Sci. U. S. A.* **82,** 3640 (1985).
37. Chukhrov, F. V., Zvyagin, B. B., Gorschkov, A. I., Yermilova, L. P., and Balashova, V. V., *Int. Geol. Rev.* **16,** 1131 (1973).
38. Treffry, A., Harrison, P. M., Cleton, M. I., de Bruijn, W. C., and Mann, S., *J. Inorg. Biochem.* **31,** 1 (1987).
39. Treffry, A., and Harrison, P. M., *Biochem. J.* **171,** 313 (1978).
40. Michaelis, L., Coryell, C. D., and Granick, S., *J. Biol. Chem.* **148,** 463 (1943).
41. Cleton, M. I., Frenkel, E. J., de Bruijn, W. C., and Marx, J. J. M., *Hepatology* **6,** 848 (1986).
42. Frenkel, E. J., van den Beld, B., and Marx, J. J. M., *Int. J. Biochem.* **17,** 421 (1985).
43. St. Pierre, T. G., Dickson, D. P. E., Webb, J., Kim, K. S., Macey, D. J., and Mann, S., *Hyperfine Interact.* **29,** 1427 (1986).

44. Wade, V. J., Levi, S., Mann, S., Treffry, A., Arosio, P., and Harrison, P. M., unpublished work.
45. Rohrer, J. S., Islam, Q. T., Watt, G. D., Sayers, D. E., and Theil, E. C., *Biochemistry* **29,** 259 (1990).
46. Hoy, T. G., and Harrison, P. M., *Br. J. Haematol.* **33,** 497 (1976).
47. Andrews, S. C., Wade, V. J., Mann, S., Guest, J. R., and Harrison, P. M., unpublished work.
48. Treffry, A., Sowerby, J.M., and Harrison, P. M., *FEBS Lett.* **100,** 33 (1979).
49. Bakker, G. R., and Boyer, R. F., *J. Biol. Chem.* **261,** 13182 (1986).
50. Lawson, D. M., Treffry, A., Artymiuk, P. J., Harrison, P. M., Yewdall, S. J., Luzzago, A., Cesareni, G., Levi, S., and Arosio, P., *FEBS Lett.* **254,** 207 (1989).
51. Treffry, A., and Harrison, P. M., *J. Inorg. Biochem.* **21,** 9 (1984).
52. Macara, I. G., Hoy, T. G., and Harrison, P. M., *Biochem. J.* **135,** 343 (1973).
53. Harrison, P. M., Andrews, S. C., Ford, G. C., Smith, J. M. A., Treffry, A., and White, J. L., *in* "Iron Transport in Microbes, Plants and Animals" (G. Winkelmann, D. van der Helm, and J. B. Neilands, eds.), p. 445. VCH Publ., Weinheim, 1987.
54. Yang, C., Meagher, A., Huynh, B. H., Sayers, D. E., and Theil, E. C., *Biochemistry* **26,** 497 (1987).
55. Treffry, A., Sowerby, J.M., and Harrison, P. M., *FEBS Lett.* **95,** 221 (1978).
56. Jacobs, D., Watt, G. D., Frankel, R. B., and Papaefthymiou, G. C., *Biochemistry* **28,** 9216 (1989).
57. Bauminger, E. R., Harrison, P. M., Nowik, I., and Treffry, A., *Biochemistry* **28,** 5486 (1989).
58. Chasteen, N. D., Antanaitis, B. C., and Aisen, P., *J. Biol. Chem.* **260,** 2926 (1985).
59. Grady, J. K., Chen, Y., and Chasteen, N. D., and Harris, D. C., *J. Biol. Chem.* **264,** 224 (1989).
60. Rosenberg, L. P., and Chasteen, N. D., *in* "Biochemistry and Physiology of Iron" (P. Saltman and J. Hegenauer, eds.), p. 405. Elsevier, New York, 1982.
61. Harrison, P. M., and Lilley, T. H., *in* "Iron Proteins and Iron Carriers" (T. M. Loehr, ed.), p. 123. VCH Publ., Weinheim, 1989.
62. Chasteen, N. D., and Theil, E. C., *J. Biol. Chem.* **257,** 7676 (1982).
63. Levi, S., Luzzago, A., Cesareni, G., Cozzi, A., Franceschinelli, F., Albertini, A., and Arosio, P., *J. Biol. Chem.* **263,** 18086 (1988).
64. Thomas, C. D., Shaw, W. V., Lawson, D. M., Treffry, A., Artymiuk, P. J., and Harrison, P. M., *Biochem. Soc. Trans.* **16,** 838 (1988).
65. Levi, S., Salfeld, F., Franceschinelli, F., Cozzi, A., Dorner, M. H., and Arosio, P., *Biochemistry* **28,** 5179 (1989).
66. Rohrer, J. S., Joo M.-S., Dartyge, E., Sayers, D. E., Fontaine, A., and Theil, E. C., *J. Biol. Chem.* **262,** 13385 (1987).
67. Rohrer, J. S., Theil, E. C., Frankel, R. B., and Papaefthymiou, G. C., *Inorg. Chem.* **28,** 3393 (1989).
68. Watt, G. D., Jacobs, D., and Frankel, R. B., *Proc. Natl. Acad. Sci. U. S. A.* **85,** 7457 (1988).
69. Artymiuk, P. J., Bauminger, E. R., Harrison, P. M., Lawson, D. M., Nowik, I., Treffry, A., and Yewdall, S. J., *in* "Iron Biominerals" (R. B. Frankel and R. P. Blakemore, eds.), p. 1. Plenum, New York, 1990.
70. Hoy, T. G., Harrison, P. M., Shabbir, M., and Macara, I. G., *Biochem. J.* **137,** 67 (1974).
71. Funk, F., Landers, J. P., Crichton, R. R., and Schneider, W., *Eur. J. Biochem.* **152,** 167 (1985).

72. Brady, M. C., Lilley, K. S., Treffry, A., Harrison, P. M., Hider, R. C., and Taylor, P. D., *J. Inorg. Biochem.* **35,** 9 (1989).
73. Arosio, P., Adelman, T. G., and Drysdale, J. W., *J. Biol. Chem.* **253,** 4451 (1978).
74. Boyd, D., Vecoli, C., Belcher, D. M., Jain, S. K., and Drysdale, J. W., *J. Biol. Chem.* **260,** 11755 (1985).
75. Stevens, P. W., Dodgson, J. B., and Engel, J. D., *Mol. Cell. Biol.* **7,** 1751 (1987).
76. Dietzel, J., Hirzmann, J., Symmons, P., Preis, D., and Kunz, W., unpublished work.
77. Leibold, E. A., and Munro, H. N., *J. Biol. Chem.* **262,** 7335 (1987).
78. Heusterspreute, M., and Crichton, R. R., *FEBS Lett.* **129,** 322 (1981).
79. Brown, A. J. P., Leibold, E. A., and Munro, H. N., *Proc. Natl. Acad. Sci. U. S. A.* **80,** 1265 (1983).
80. Costanzo, F., Santoro, C., Colantuoni, V., Bensi, G., Raguei, G., Romano, V., and Cortese, R., *EMBO J.* **3,** 23 (1984).
81. Jain, S. K., Barett, K. J., Boyd, D., Favreau, M. F., Crampton, J., and Drysdale, J. W., *J. Biol. Chem.* **260,** 11762 (1985).
82. Collawn, J. F., Gowan, L. K., Crow, H., Schwabe, C., and Fish, W. W., *Arch. Biochem. Biophys.* **259,** 105 (1987).
83. Beaumont, C., Dugast, I., Renaudie, F., Souroujon, M., and Granchamp, B., *J. Biol. Chem.* **264,** 7498 (1989).
84. Laulhere, J.-P., Laboure, A.-M., and Briat, J.-F., *J. Biol. Chem.* **264,** 3629 (1989).
85. Andrews, S. C., Smith, J. M. A., Guest, J. R., and Harrison, P. M., *Biochem. Biophys. Res. Commun.* **158,** 489 (1989).
86. Andrews, S. C., Findlay, J. B. C., Guest, J. R., Harrison, P. M., Keen, J., and Smith, J. M. A., unpublished work.
87. Kurokawa, T., Fukomori, Y., and Yamanata, T., *Biochim. Biophys. Acta* **976,** 135 (1989).
88. Harker, A. R., and Wullstein, L. H., *J. Bacteriol.* **162,** 651 (1985).
89. Harrison, P. M., *J. Mol. Biol.* **1,** 6 (1959).
90. Hoy, T. G., Harrison, P. M., and Hoare, R. J., *J. Mol. Biol.* **86,** 301 (1974).
91. Fischbach, F. A., Harrison, P. M., and Hoy, T. G., *J. Mol. Biol.* **39,** 235 (1969).
92. Harrison, P. M., *J. Mol. Biol.* **6,** 404 (1963).
93. Rice, D. W., Dean, B., Smith, J. M. A., White, J. L., Ford, G. C., and Harrison, P. M., *FEBS Lett.* **181,** 165 (1985).
94. Lawson, D. M., Ph.D Thesis, University of Sheffield (1990).
95. Smith, J. M. A., Ford, G. C., and Harrison, P. M., *Biochem. Soc. Trans.* **16,** 836 (1988).
96. Smith, J. M. A., Ford, G. C., Harrison, P. M., Yariv, J., and Kalb, A. J., *J. Mol. Biol.* **205,** 465 (1989).
97. Smith, J. M. A., Andrews, S. C., Guest, J. R., and Harrison, P. M., *in* "Iron Biominerals" (R. B. Frankel and R. P. Blakemore, eds.), p. 325. Plenum, New York, 1990.
98. Andrews, S. C., Harrison, P. M., and Guest, J. R., *J. Bacteriol.* **171,** 3940 (1989).
99. Andrews, S. C., Smith, J. M. A., Guest, J. R., and Harrison, P. M., *Biochem. Soc. Trans.* **18,** 658 (1990).
100. Yewdall, S. J., Lawson, D. M., Artymiuk, P. J., Treffry, A., Harrison, P. M., Luzzago, A., Cesareni, G., Levi, S., and Arosio, P., *Biochem. Soc. Trans.* **18,** 1028 (1990).
101. Smith, J.M. A., Stansfield, R. F. D., Ford, G. C., White, J. L., and Harrison, P. M., *J. Chem. Educ.* **65,** 1083 (1988).
102. Bourne, P. E., Harrison, P. M., Lewis, W. G., Rice, D. W., Smith, J. M. A., and

Stansfield, R. F. D., *in* "The Biochemistry and Physiology of Iron" (P. Saltman and J. Hegenauer, eds.), p. 345. Elsevier/North-Holland, New York, 1982.
103. Weber, P. C., and Salemme, F. R., *Nature (London)* **287,** 83 (1980).
104. Scott Matthews, F., *Prog. Biophys. Mol. Biol.* **45,** 1 (1985).
105. Cheesman, M. R., Thomson, A. J., Greenwood, C., Moore, G. R., and Kadir, F., *Nature (London)* **346,** 771 (1990).
106. Harrison, S. C., and Blout, E. R., *J. Biol. Chem.* **240,** 299 (1965).
107. Wagstaff, M., Worwood, M., and Jacobs, A., *Biochem. J.* **173,** 969 (1978).
108. Yewdall, S. J., Lawson, D. M., Artymiuk, P. J., Treffry, A., Luzzago, A., Cesareni, G., Levi, S., Arosio, P., and Harrison, P. M., unpublished work.
109. Treffry, A., Harrison, P. M., Luzzago, A., and Cesareni, G., *FEBS Lett.* **247,** 268 (1989).
110. Harrison, P. M., Treffry, A., and Lilley, T. H., *J. Inorg. Biochem.* **278,** 287 (1986).
111. Levi, S., Arosio, P., Franceschinelli, F., Cozzi, A., Santambrogio, P., Luzzago, A., and Cesareni, G., *Int. Conf. Proteins Iron Transp. Storage, 9th,* July, p. 81 (1989).
112. Bauminger, E., Cesareni, G., Harrison, P. M., Luzzago, A., Nowik, I., and Treffry, A., unpublished work.
113. Massover, W. H., *J. Mol. Biol.* **123,** 721 (1978).
114. Williams, R. J. P., *in* "Frontiers in Bio-inorganic Chemistry" (A. V. Xavier, ed.), p. 431. VCH Publ., Weinheim, 1986.
115. Lawson, D. M., Artymiuk, P. J., Yewdall, S. J., Smith, J. M. A., Livingstone, J. C., Treffry, A., Luzzago, A., Levi, S., Arosio, P., Cesareni, G., Thomas, C. D., Shaw, W. V., and Harrison, P. M. *Nature (London)* (in press).